Stratospheric and tropospheric NO2 variability on the diurnal and annual scale: a combined retrieval from ENVISAT/SCIAMACHY and solar FTIR at the Permanent Ground-Truthing Facility Zugspitze/Garmisch

R. Sussmann, W. Stremme, J. P. Burrows, A. Richter, W. Seiler, M. Rettinger

Atmos. Chem. Phys., 5, 2657–2677, 2005
www.atmos-chem-phys.org/acp/5/2657/
SRef-ID: 1680-7324/acp/2005-5-2657
European Geosciences Union

Atmospheric Chemistry and Physics

Stratospheric and tropospheric NO_2 variability on the diurnal and annual scale: a combined retrieval from ENVISAT/SCIAMACHY and solar FTIR at the Permanent Ground-Truthing Facility Zugspitze/Garmisch

R. Sussmann[1], **W. Stremme**[1], **J. P. Burrows**[2], **A. Richter**[2], **W. Seiler**[1], **and M. Rettinger**[1]

[1]IMK-IFU, Forschungszentrum Karlsruhe, Garmisch-Partenkirchen, Germany
[2]Institute of Environmental Physics, University of Bremen, Bremen, Germany

Received: 15 March 2005 – Published in Atmos. Chem. Phys. Discuss.: 20 April 2005
Revised: 26 July 2005 – Accepted: 23 September 2005 – Published: 7 October 2005

Abstract. Columnar NO_2 retrievals from solar FTIR measurements at the Zugspitze (47.42° N, 10.98° E, 2964 m a.s.l.), Germany were investigated synergistically with columnar NO_2 retrieved from SCIAMACHY data by the University of Bremen scientific algorithm UB1.5 for the time span July 2002–October 2004. A new concept to match FTIR data to the time of satellite overpass makes use of the NO_2 daytime increasing rate retrieved from the FTIR data set itself [+1.02(6) E+14 cm^{-2}/h]. This measured increasing rate shows no significant seasonal variation. SCIAMACHY data within a 200-km radius around Zugspitze were considered, and a pollution-clearing scheme was developed to select only pixels corresponding to clean background (free) tropospheric conditions, and exclude local pollution hot spots. The resulting difference between SCIAMACHY and FTIR columns (without correcting for the different sensitivities of the instruments) varies between 0.60–1.24 E+15 cm^{-2} with an average of 0.83 E+15 cm^{-2}. A day-to-day scatter of daily means of ≈7–10% could be retrieved in mutual agreement from FTIR and SCIAMACHY. Both data sets are showing sufficient precisions to make this assessment. Analysis of the averaging kernels gives proof that at high-mountain-site FTIR is a highly accurate measure for the pure stratospheric column, while SCIAMACHY shows significant tropospheric sensitivity. Based on this finding, we set up a combined a posteriori FTIR-SCIAMACHY retrieval for tropospheric NO_2, based upon the averaging kernels. It yields an annual cycle of the clean background (free) tropospheric column (<10 km) with variations between 0.75–1.54 E+15 cm^{-2}, an average of 1.09 E+15 cm^{-2}, and an intermediate phase between that of the well known boundary layer and stratospheric annual cycles. The outcome is a concept for an integrated global observing system for tropospheric NO_2 that comprises DOAS nadir satellite measurements and a set of latitudinally distributed mountain-site or clean-air FTIR stations.

Correspondence to: R. Sussmann
(ralf.sussmann@imk.fzk.de)

1 Introduction

The importance of NO_2 in atmospheric chemistry had been described in the literature more than 25 years ago (Crutzen, 1979). Long-term research has been performed since then aiming at a better understanding of its differing role in the determination of the earth's ozone distribution in the stratosphere (catalytic ozone destruction), and the troposphere (ozone formation via photochemical smog). While the main sources and source regions of NO_2 are known, large uncertainties remain on the individual source strengths and their latitudinal and seasonal variations (IPCC, 2001).

Interest in the climatic role of tropospheric NO_2, however, has shown up only recently, when it has been found that a significant radiative forcing (exceeding that of CO_2) can build up during periods with extremely elevated NO_2 levels in the troposphere (Solomon et al., 1999). Such pollution events might be underestimated in duration and horizontal extension due to the short lifetime of NO_2 in the boundary layer: However, it was shown only recently that NO_2-rich pollution hot spots can spread over large areas for several days (Leue et al., 2001), and that NO_2 transport over large distances is possible (Stohl et al., 2003; Schaub et al., 2005).

Tropospheric NO_2 hot spots and source strengths and their quantification in time and space can be investigated using modern nadir-looking satellite instruments like GOME,

SCIAMACHY, or OMI (Borell et al., 2004; Levelt et al., 2000). Satellite based retrievals of tropospheric NO_2 have to account for the stratospheric contribution which has been done by different approaches. The reference sector method makes use of unpolluted columns above the ocean as a reference (e.g., Richter and Burrows, 2002) and thus assumes negligible tropospheric NO_2 over the Pacific between 180° and 190° longitude, as well as longitudinal homogeneity of the stratospheric NO_2 layer. However, close to the Polar Vortex or during major changes in stratospheric dynamics, this approximation is introducing some artifacts at high latitudes in winter and spring. Further approaches like image processing techniques (e.g., Leue et al., 2001), or assimilation into a chemistry transport model (Boersma et al., 2004) have been applied. Another method would be to use independent data such as the SCIAMACHY limb measurements (Bovensmann et al., 1999) or, as explored in this paper, simultaneous ground-based measurements.

First comparisons of satellite derived tropospheric NO_2 with air borne profile and column measurements (Heland et al., 2002; Martin et al., 2004; Heue et al., 2005) showed good agreement for homogeneous situations, but in the presence of spatial gradients, differences with respect to ground-based measurements can be large (Petritoli et al., 2004). Error estimates for the satellite data are about 50% for polluted regions and larger in clean regions (Richter and Burrows, 2002; Boersma et al., 2004). Obviously, the current satellite retrievals of tropospheric NO_2 are still of limited accuracy. Therefore intensive further joint investigations together with ground-based measurements are required targeting at both validation and synergistic use, i.e., an improved error assessment as well as an improvement of the satellite measurements themselves, by synergistically combining them with the complementary information attainable from ground-based measurements.

For this purpose in general terms (dealing with a variety of further trace species, satellite missions, and ground-based instrumentation), a Permanent Ground-Truthing Facility has been built up at the NDSC (Network for the Detection of Stratospheric Change) Primary Station Zugspitze/Garmisch, Germany according to the requirements of the World Meteorological Organization (WMO, 2000). It is equipped with a variety of ground-based remote sounding instrumentations, and aims at performing operational satellite validation and promoting the synergistic use of satellite and ground-based measurements (Sussmann, 2004).

Subject of this paper is validation and synergistic use of ground-based solar FTIR measurements of NO_2 performed at the Zugspitze together with ENVISAT/SCIAMACHY measurements (Bovensmann et al., 1999). There are three issues which have to be properly taken into account before a direct comparison is possible: i) The stratospheric NO_2 diurnal cycle hinders a direct comparison with FTIR measurements, which are recorded not exactly at the time of satellite overpass, ii) the high horizontal variability of boundary layer NO_2 makes it difficult to compare ground-based data taken at one location to satellite data within a certain selection radius around that site, and, iii) the different sensitivity of SCIAMACHY versus FTIR to tropospheric NO_2 has to be taken into account.

While these issues have been discussed qualitatively in many validation studies (Lambert et al., 1999; 2004; Richter et al., 2004; Sussmann et al., 2004a, b) this paper gives a quantitative treatment for validation by FTIR for the first time. This is done by i) applying a new concept for deriving virtual coincidences from the individual daily FTIR measurements to the time of ENVISAT overpass (Sect. 2), and ii) using all SCIAMACHY data within a selection radius of 200-km around the Zugspitze and applying a new pollution-clearing scheme for exclusion of local pollution hot spots (Sect. 3).

The quantitative treatment of the different sensitivities of SCIAMACHY versus FTIR to tropospheric NO_2 leads us to two limiting cases: i) Observed differences (satellite to ground) are only due to inherent errors in either of the two remote sounding data sets under the simplifying assumption that the two measurement systems have identical sampling characteristics or, ii) the observed differences can be attributed only to the different sampling characteristics of the two instruments under the assumption that they are both working in principle without intrinsic errors. Reality will be in between these limiting cases, and, therefore, we investigated both of them in parallel. Consequently, first a classical direct intercomparison of the times series of SCIAMACHY and FTIR NO_2 columns is given (Sect. 4).

The crucial part of this paper is then presented in Sect. 5. Here we make use of the differing averaging kernels (different sensitivities) of FTIR and SCIAMACHY and iterate (free) tropospheric NO_2 levels in order to match FTIR and SCIAMACHY data together. This results in the first (a posteriori) retrieval of tropospheric NO_2 from the combined use of FTIR and satellite data. The result will be discussed in terms of geophysical relevance. Section 6 gives the conclusions with an outlook on how to improve satellite based retrievals of tropospheric NO_2 by an integrated global observing system based on nadir-looking satellite instruments and mountain-site or clean-air FTIR stations.

2 The FTIR NO_2 columns data set

2.1 FTIR measurements

Ground-based data are being recorded by the NDSC-Primary Status solar FTIR instrument at the Zugspitze (47.42° N, 10.98° E, 2964 m a.s.l.) continuously since 1995. The Zugspitze-FTIR instrument and retrieval set-up has been described in detail elsewhere (Sussmann et al., 1997; Sussmann, 1999). Briefly, a high-resolution Bruker IFS 120 HR Fourier Transform Spectrometer is operated with an actively

controlled solar tracker, and liquid-nitrogen cooled MCT (HgCdTe) and InSb detectors. The FTIR data set used for this study covers the time span from 23 July 2002 to 21 September 2004 and comprises 914 InSb spectra (after elimination of bad spectra by quality control) recorded on 200 measurement days, i.e., 4.6 spectra per measurement day on average. Each spectrum resulted from averaging 5 scans with a maximum optical path difference of 175 cm (integrated within 10 min).

2.2 FTIR column retrieval

The Zugspitze NO_2 retrieval utilizes the prominent absorption peak at 2914.65 cm^{-1} initially suggested by Camy-Peyret et al. (1983), which is a multiplet of several closely spaced and not spectrally resolved transitions. The wide micro-window used (2914.51–2914.86 cm^{-1}) intentionally includes the wing of the strong CH_4 line at 2914.50 cm^{-1} which is retrieved simultaneously to avoid cross correlations. Columns are retrieved using the non-linear least squares spectral fitting software SFIT2 (version 3.90) initially developed at NASA Langley Research Center and NIWA (Pougatchev et al., 1995). We did not perform a profile retrieval, because the weak NO_2 absorption feature does not allow to infer altitude-resolved information. In other words, the number of degrees of freedom of signal (dofs) of the retrieval, i.e., the trace of the averaging kernel matrix (Rodgers, 1998) will always be in the order of 1 setting up the a priori covariance matrix (or its inverse) in various reasonable forms. Therefore we applied a simple (Tikhonov-regularization type) hard smoothness constraint, leading to dofs $\equiv$1, i.e., a volume mixing ratio (VMR) profile scaling. The resulting total column averaging kernels are presented in Sect. 5.1 below. As a priori the 1976 US Standard NO_2 VMR profile (Anderson et al., 1986) was used with the tropospheric part up to 10 km altitude set to zero. This profile will be referred to thereafter as "reduced US Standard profile". The reason for this choice is detailed below. Daily p-T-profiles from the Munich radio sonde station (located 80 km to the north of the Zugspitze) have been utilized and the HITRAN-2004 molecular line parameters compilation was used; see Rothmann et al. (2003) for a description of the previous version.

Error estimates for the NO_2 column retrievals from the 2914.65 cm^{-1} feature by FTIR have already been presented by Camy-Peyret et al. (1983), Flaud et al. (1983, 1988), and Rinsland et al. (1988). Individual measurement precisions of $\approx$10% have been reported as well as accuracies of $\approx$10% been given. Rinsland et al. (2003) have pointed to a possible significant a priori contribution to the retrievals. In extension to these previous error assessments we will thereafter investigate quantitatively in full detail the impact of differing HITRAN versions, differing a priori VMR profiles, as well as the influence of the averaging kernels on the FTIR column retrievals of NO_2.

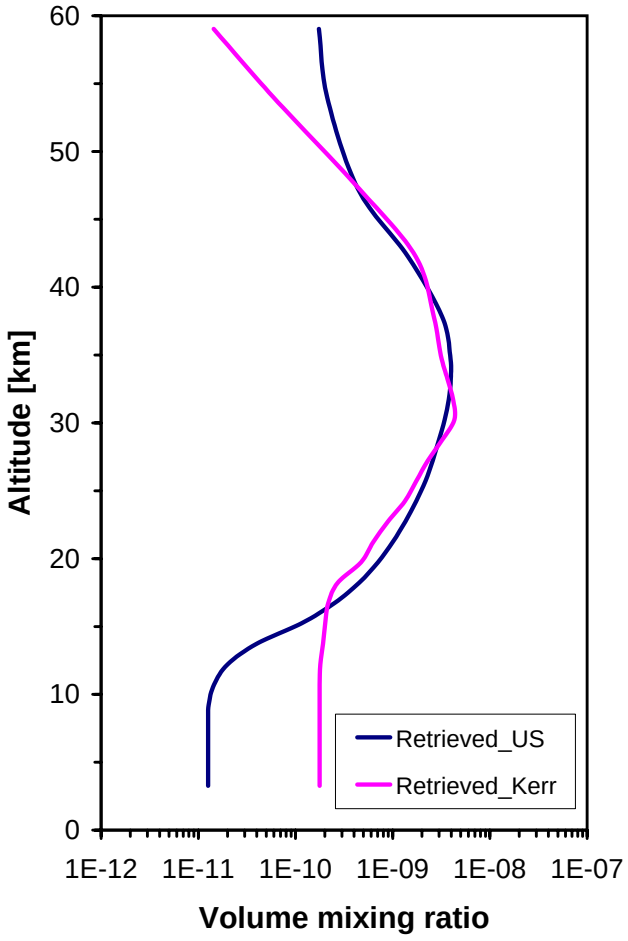

Fig. 1. NO_2 FTIR (profile scaling) retrieval results from one arbitrarily chosen measured Zugspitze FTIR spectrum with SZA=61° using two different NO_2 a priori VMR profiles, i.e., the 1976 US Standard atmosphere (blue) versus the retrieval based upon the standard profile by "Kerr et al." (Rinsland, personal communication, 1999), distributed with the "refmod99" data set (magenta).

2.3 Impact of line parameter errors on FTIR retrievals

In order to add up-to-date information on the impact of line parameter errors on the absolute accuracy of the NO_2 columns, we retrieved the whole FTIR data set of this study with the three most recent HITRAN versions, i.e., HITRAN 2000, HITRAN 2000 with update V11.0 9/2001, as well as HITRAN 2004, which is used throughout this study. Using HITRAN 2004 as a reference, we found the following relative changes for overall averages of the columns: HITRAN2004/HITRAN 2000=1.0003 and HITRAN2004/HITRAN 2000(9/2001 update)=1.0385. We conclude that the uncertainty of the line parameters could introduce a bias on the retrieved FTIR columns that is probably on the few per cent (<5%) level.

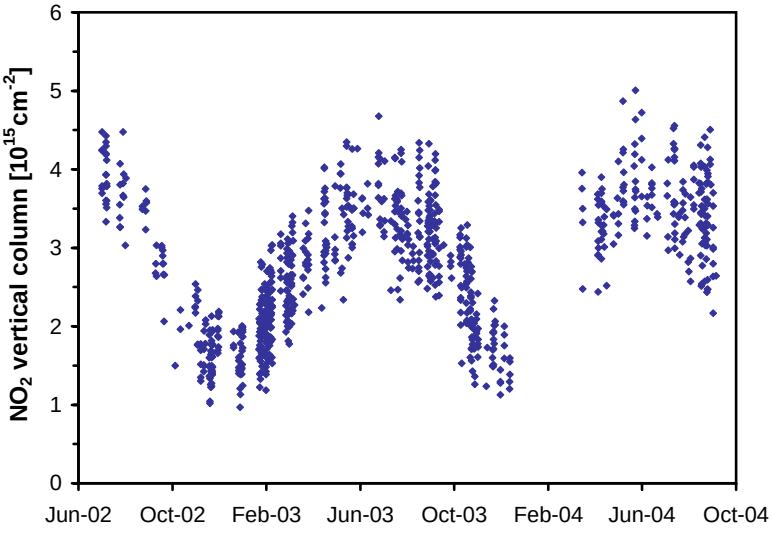

Fig. 2. The Zugspitze FTIR NO_2-vertical column data set analyzed in this study for SCIAMACHY validation by using as a priori the US 1976 Standard NO_2 VMR profile with the tropospheric part (<10 km) set to zero. Plotted are columns retrieved from individual measurements (10-min integration time).

Table 1. FTIR NO_2 column retrieval results from one arbitrarily chosen measured spectrum with SZA=61° using two different a priori profiles, i.e., the NO_2 profile of the 1976 US Standard atmosphere (US) versus the standard profile by "Kerr et al." (Rinsland, personal communication, 1999), distributed with the "refmod99" data set (Kerr).

	US	Kerr	Kerr – US
Total Column (Ground–100 km)	3.04 E+15	4.67 E+15	1.63 E+15
Partial Column (10–100 km)	2.92 E+15	3.02 E+15	0.10 E+15
Partial Column (Ground–10 km)	0.12 E+15	1.65 E+15	1.53 E+15

2.4 Impact of a priori VMR profiles on FTIR retrievals

Figure 1 shows two different FTIR retrieval results from the same arbitrarily chosen spectrum {solar zenith angle (SZA)=61°} using two different a priori profiles, i.e., the 1976 US Standard NO_2 profile, and the profile designated as "Kerr et al." within the so-called "refmod99" data set distributed by Rinsland (personal communication, 1999). The latter yields a significantly higher (54%) total column retrieved from the same spectrum (see Table 1). Table 1 also shows that the stratospheric columns are nearly the same for both retrievals and the difference is mainly in the tropospheric columns. This result can be understood by the different relative shape of these a priori profiles, i.e., the much higher tropospheric contribution of the "Kerr et al." profile with its tropospheric column being a considerable fraction of the total column, together with a reduced tropospheric sensitivity of the FTIR retrieval compared to the stratospheric sensitivity: Obviously, any real perturbation in the stratosphere relative to the a priori will lead to analogous scaling of the tropospheric part of the a priori profile, independently from whether there is a real perturbation or not. This effect is described in a quantitative way using the total column averaging kernels in Sect. 5.2.

So we find the choice of the magnitude of the tropospheric part of the a priori VMR profile to be the potentially dominant biasing contribution, if the corresponding tropospheric column makes up a considerable fraction of the total column.

As a consequence for validation and synergistic use within this study we adopted the same a priori profile for the FTIR retrievals as are used for the satellite retrievals, i.e., the reduced US Standard NO_2 profile.

2.5 FTIR individual columns time series

The FTIR NO_2 columns data set used for this study is plotted in Fig. 2. Plotted are columns retrieved from individual measurements. As we will infer from our sensitivity study in Sect. 5.2, the FTIR columns are a good measure for the stratospheric column and are only weakly (if at all) influenced by tropospheric pollution events. As a consequence, Fig. 2 displays a clear annual cycle which is due to the seasonal changes in day length and thus photolysis and to a lesser degree also temperature. The daily scatter of the individual column measurements is dominated by the diurnal cycle as investigated in the next section.

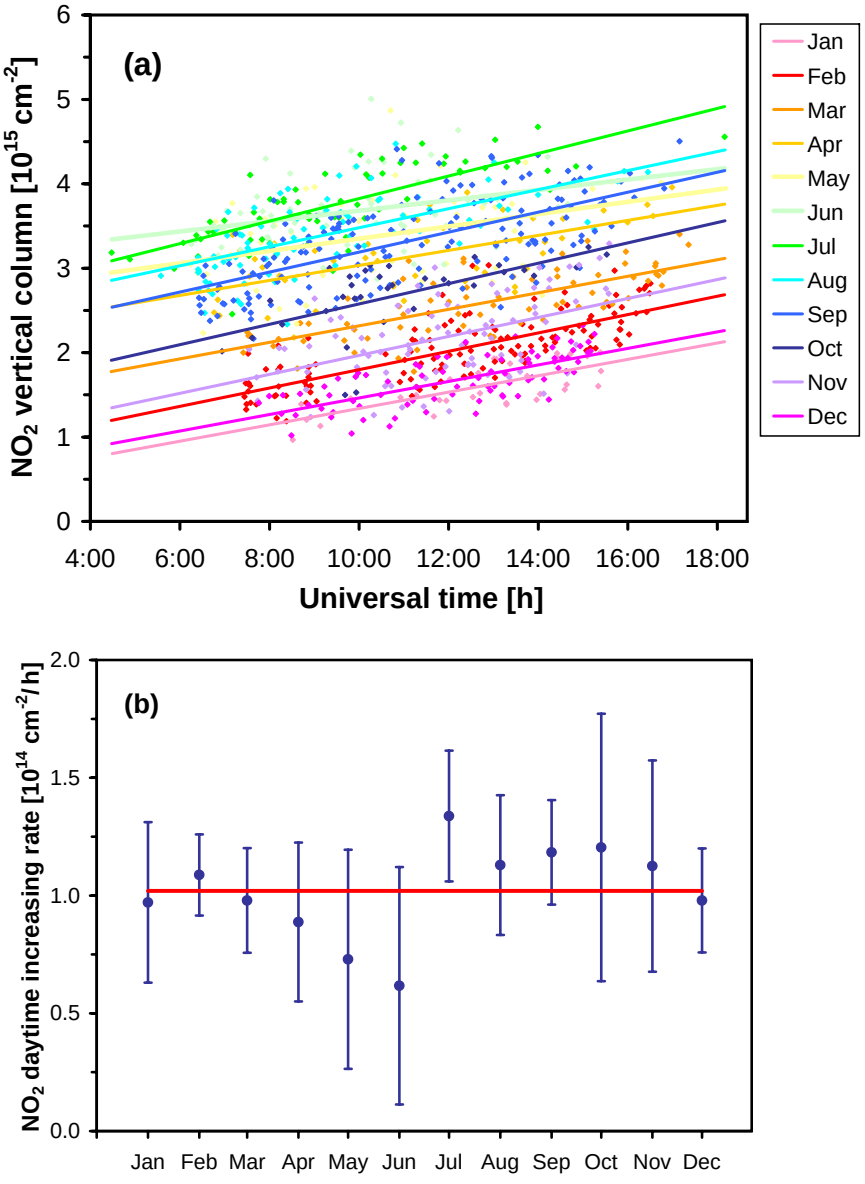

Fig. 3. (a) The Zugspitze FTIR NO_2-vertical column data set as shown in Fig. 2, but plotted as a function of the time of the day. Data were classified into 12 months and linear fits to the diurnal increase performed on the monthly data sets. **(b)** The 12 different diurnal increasing rates obtained from the fits performed to the monthly FTIR data sets in (a). The plotted slope error bars (2 sigma) are obtained from the linear fits in (a), and the red line gives the average increasing rate, i.e., 1.02(6) E+14 cm^{-2}/h.

2.6 The stratospheric NO_2 daytime increasing rate as a function of season inferred from FTIR

Stratospheric total NO_2 has a well defined diurnal cycle with a daytime increasing rate that has been described experimentally only by a few individual days of FTIR measurements up to now (Flaud et al., 1983, 1988; Rinsland et al., 1988). The daytime increasing rate has been discussed with respect to the consequences for satellite validation with ground-based zenith-sky DOAS instruments by Lambert et al. (1999, 2004).

We reinvestigated the NO_2 daytime increasing rate using the full FTIR data set of this study. Figure 3a shows all individual FTIR columns of the data set, but now plotted as function of the hour of the day, and separated for the 12 different months by colors. For each month a linear fit is performed to all the individual columns of this month.

Fig. 3b gives evidence, that there is no significant seasonal change of the daytime increasing rate of stratospheric NO_2 within the FTIR error bars. This result is obtained for the Zugspitze located at 47° N and should be representative for mid latitudes. It is of some interest since it had been argued

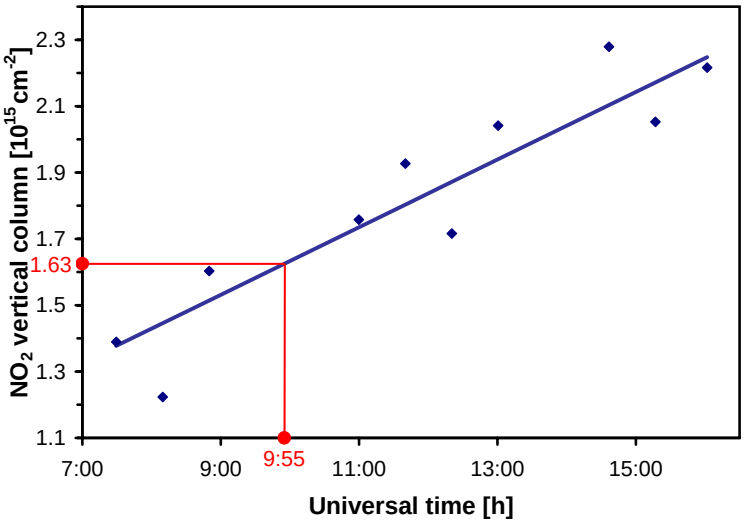

Fig. 4. Zugspitze FTIR NO_2 vertical column data – individual measurements of one arbitrarily chosen day. The blue line is a fit with a constant slope (i.e., the daytime increasing rate of 1.02 E+14 cm^{-2}/h) with only the offset as fit parameter. The red lines illustrate the concept of the "virtual-coincidence column", here for a 09:55 UT satellite overpass. For details, see text.

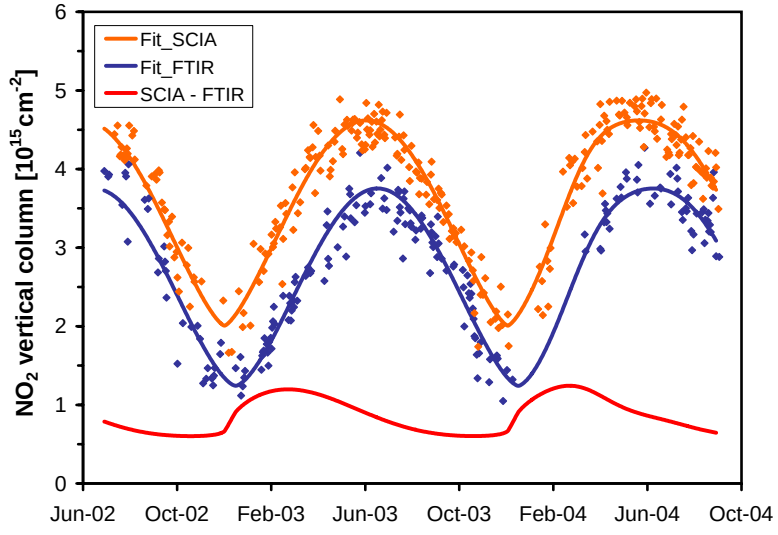

Fig. 5. Blue: The Zugspitze FTIR NO_2-vertical column data set as in Fig. 2, but now the daily virtual-coincidence columns for the time of ENVISAT overpass are plotted. Orange: SCIAMACHY NO_2-vertical column data, i.e., daily averages of the pollution-cleared data (see Fig. 7c) are plotted. Red: Difference between orange and blue line. Mathematical details of the analytic function that has been fitted to both data sets (solid lines) are described in Appendix A.

from experiments with a stratospheric photochemical model that the daytime variation should be a function of the season since the build up of N_2O_5 depends on the length of the night and because its rate of photo dissociation varies with solar elevation (Flaud et al., 1983).

Since there is no significant seasonal dependence of the daytime increasing rate we infer from the 12 individual monthly rates of Fig. 3b one annual average rate. The resulting daytime NO_2 increasing rate is 1.02(6) E+14 cm^{-2}/h.

2.7 The concept of virtual-coincidence columns for FTIR data

Individual FTIR measurements are recorded sequentially and are distributed in time over the whole day. Thus, the individual FTIR columns of each day vary according to the diurnal increase. On the other hand, the individual SCIAMACHY measurements for one day (all pixels within a 200-km selection radius around Zugspitze) are all recorded nearly at the same time, i.e., the time of overpass, which is roughly at 10:00 UT.

Table 2. Statistics of NO_2 data scatter for FTIR and SCIAMACHY UB1.5 measurements. SCIAMACHY data were taken within a 200-km pixel-selection radius around the Zugspitze for each day, and both cloud clearing and a pollution clearing has been applied to the data as described in the text. The index for the number of measurement days is i. First column: $AV_i(n_i)$, i.e., average of the numbers n_i of individual measurements during each measurement day. Second column: $AV_i(\sigma_i)$, i.e., average of the "single-value standard deviations" calculated from the individual measurements for the different days. For FTIR each standard deviation is calculated relative to the daily fit (vertical offset as fit parameter) to the daytime increase with constant slope of 1.02(6) E+14 cm^{-2}/h. 3rd column: $AV_i(\sigma_i/\mathrm{sqrt}(n_i))$, i.e., average of the "standard deviations of the daily mean values" calculated from the individual measurements for the different days. (Again for FTIR each value is calculated relative to the daily fitted line describing the diurnal increase.) 4th column: Standard deviations of daily means calculated from the daily-means data sets as shown in Fig. 5, i.e., relative to the analytic function fitted to the annual cycle (functional fit described in Appendix A).

	$AV_i(n_i)$	$AV_i(\sigma_i)$	$AV_i(\sigma_i/\mathrm{sqrt}(n_i))$	σ of daily means corrected for ann. cycle and pollution (Fig. 5)
Zugspitze FTIR	4.6	8.8%	4.3%	9.2%
SCIAMACHY	22	6.8%	1.9%	6.5%

Therefore, we have to match the individual measurement times of FTIR to the time of ENVISAT overpass. Our concept to achieve this is presented in Fig. 4. For each measurement day we fitted a line with a constant slope (i.e., the daytime increasing rate of 1.02 E+14 cm^{-2}/h) to the retrieved FTIR columns, and only the vertical offset was used as a fitting parameter. Subsequently, the column was read out from this fitted line at the exact time of the daily overpass. This is what we will refer to as "virtual-coincidence column" thereafter, since it is constructed for the time of overpass which usually does not coincide with the time of a real FTIR measurement.

We give a conservative estimate of the propagation of the error of the daytime increasing rate (0.06 E+14 cm^{-2}/h, see above) into the virtual coincidence column as follows. Assuming that there is only one late-evening FTIR measurement at 19:00 UT, i.e., 9 h after the 10:00 UT satellite overpass, the error of the daytime increasing rate would then result in an error of the virtual coincidence column of 9 h × 0.06 E+14 cm^{-2}/h=0.54 E+14 cm^{-2}, which would be ≈1% for a typical summer column level of 4.5 E+15 cm^{-2}. In analogy, we estimate for a winter-evening FTIR measurement at 15:00 UT a 5 h × 0.06 E+14 cm^{-2}/h=0.3 E+14 cm^{-2} error which would be ≈1.5% for a typical winter column level of 2 E+15 cm^{-2}.

2.8 Functional fit to daily FTIR data

The FTIR daily virtual-coincidence columns are plotted in Fig. 5. The figure also shows a fit to these data using the analytic function described in Appendix A.

This functional fit was performed for two reasons as described in our previous work (Sussmann and Buchwitz, 2005; Sussmann et al., 2005): i) In order to be able to compare FTIR to SCIAMACHY results even in case of alternating data gaps, and ii) to be able to calculate a standard deviation of the daily virtual-coincidence columns around the functional fit (describing the annual cycle), for a characterization of the day-to day scatter.

2.9 Characterization of the daily scatter of FTIR NO_2 columns

First we want to characterize the precision of individual FTIR column measurements. For this purpose we have to derive statistical quantities with the scattering effect due to the stratospheric NO_2 daytime increase eliminated. This is performed using the concept of Fig. 4. For each day with index i and n_i measurements, the standard deviation σ_i and the standard deviation of the mean value $\sigma_i/\mathrm{sqrt}(n_i)$ were calculated relative to the line fitted to the daytime increase, and subsequently the average (AV) of these quantities over all days was derived. The resulting $AV_i(\sigma_i)$=8.8% is a measure for the precision of individual FTIR column measurements. $AV_i(\sigma_i/\mathrm{sqrt}(n_i))$=4.3% is a measure for the precision of the virtual-coincidence column (Table 2).

Finally, we calculate a standard deviation of the daily virtual-coincidence columns around the function fitted to the annual cycle. This leads to a standard deviation of σ=9.2%, see Table 2. This value comprises both the precision of a daily virtual-coincidence column as well as the day-to-day scatter, and is significantly higher than the precision of a daily virtual-coincidence column alone (4.3%). Therefore the day to-day scatter can be detected by FTIR significantly and is probably in the order of 10%. This day to day scatter should be a measure of the true stratospheric variability of NO_2. Although this is dominated by photolysis, there is also a dependence on the origin of the probed airmass, e.g., spring-time variability can be caused by the change in circulation.

3 The SCIAMACHY UB1.5 columns data set

3.1 SCIAMACHY measurements

The SCanning Imaging Absorption spectroMeter for Atmospheric CHartographY (SCIAMACHY) was launched on ENVISAT into a sun-synchronous orbit with a 10:00 LT equator crossing time on 1 March 2002. SCIAMACHY is an 8 channel UV/visible/NIR grating spectrometer covering the wavelength region of 220 to 2400 nm with 0.2–1.5 nm spectral resolution depending on wavelength (Bovensmann et al., 1999). Along one orbit, the instrument performs alternating nadir and limb measurements, facilitating profile retrievals from the Mesosphere to the UT/LS region and also column measurements. In addition, solar and lunar occultation measurements are performed under certain conditions, as well as a solar irradiance measurement once per day. The UV/vis nadir measurements of SCIAMACHY are performed with a high horizontal resolution of up to $30\times30\,km^2$. Global coverage at the equator is achieved in 6 days and more frequently at higher latitudes. Nadir data used for the total column NO_2 retrievals are available since August 2002.

3.2 SCIAMACHY UB1.5 column retrieval

In previous work we validated the ESA operational near-real-time NO_2 total column data product, versions 5.01 and 5.02 (Sussmann et al., 2004a, b). We found a significant problem of this processor in reproducing the annual cycle, i.e., the fall decrease of the columns was strongly underestimated, which is probably due to reading out (too high) climatological tropospheric columns into the retrieval data set in case of cloudy pixels. In comparison we found that the scientific algorithm of the University of Bremen (UB1.5) was able to reproduce the annual cycle properly (Sussmann et al., 2004b). Therefore, we are dealing thereafter with the University of Bremen algorithm only.

The UB1.5 algorithm is an adaptation of the GOME retrieval (Richter and Burrows, 2002). Details of this adaptation have been described by Richter et al. (2004). Briefly, the wavelength window 425–450 nm in channel 3 was chosen for the fit, and a constant correction of $1.0\,E{+}15\,cm^{-2}$ was added to the slant columns as an empirical correction inferred from early validation, which translates to a vertical column offset of $0.05–0.5\,E{+}15\,cm^{-2}$. The background spectrum used in the slant column fitting is the azimuth scan mirror diffuser spectrum recorded on 15 December 2002. The results of the DOAS retrievals are slant column densities (SCD) that correspond to the column of molecules integrated along the effective light path through the atmosphere. To convert these into a vertical column density (VCD), an airmass factor (AMF) is applied that corrects for the light path enhancement. (Note that due to the infrared spectral domain for the FTIR retrievals the AMF is solely determined by the air density and the geometrical cosine-correction including refraction.) The UV-DOAS AMF are a function of solar zenith angle, the instrument line of sight, the relative azimuth between viewing direction and the sun, but also depends on the vertical profile of NO_2 and parameters such as surface albedo, aerosol loading or clouds.

3.3 The a priori profile for SCIAMACHY UB1.5 retrievals

We have shown for the FTIR retrievals that the accurate determination of the total NO_2 column depends heavily on a priori assumptions on the vertical VMR profile that is not available from the measurements and therefore introduces significant biases (Table 1). The same is true in a related manner for the SCIAMACHY UB1.5 retrievals. Therefore, as an alternative approach, for the SCIAMACHY UB1.5 retrievals, a purely stratospheric AMF is calculated based on the US Standard atmosphere after removing the tropospheric part and assuming a surface albedo of 5%, and only stratospheric background aerosols (Richter et al., 2004). The columns retrieved with this AMF, are expected to give a good measure for the true stratospheric column for clean regions but will significantly exceed the true stratospheric column in polluted regions. At the same time, the retrieved column will slightly underestimate the true total column in clean regions, and significantly underestimate the true total column in polluted regions. A quantitative analysis of these effects by using the concept of averaging kernels will be presented in Sect. 5.2.

3.4 Scientific SCIAMACHY UB1.5 columns: full data set and cloud clearing

The SCIAMACHY NO_2 columns data set retrieved by the UB1.5 algorithm at the University of Bremen for a 200-km radius around the Zugspitze is shown in Fig. 6. Plotted are columns retrieved from all individual measurements (grey), as well as a reduced data set (orange) which resulted from application of a cloud clearing scheme. We applied a simple intensity threshold which leads to an effective clearing of both cloud and snow covered pixels. This data set will be exclusively utilized throughout this paper thereafter.

The figure displays a clear annual cycle for the daily minimum values whereas the daily maxima are spiking to very high values frequently. Note from Fig. 6 that by the cloud clearing the highest spikes of the full data set have been eliminated. This can be understood in terms of the strongly enhanced sensitivity to tropospheric pollution above snow or clouds.

Obviously, quite often strong regional boundary layer pollution events occur within the 200-km selection radius around Zugspitze. The retrieved SCIAMACHY columns are a reasonable measure of both the stratospheric and total column for clean conditions, and are significantly impacted by boundary layer pollution events, although they strongly underestimate boundary pollution enhancements in

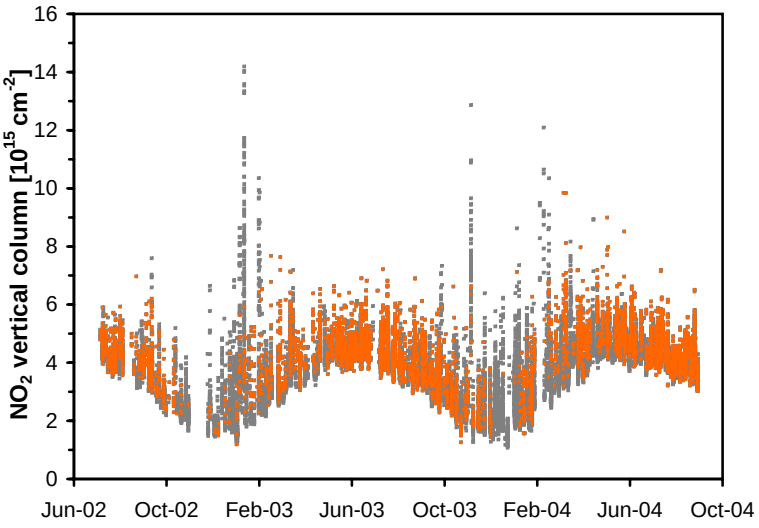

Fig. 6. The SCIAMACHY NO_2 vertical column data set analyzed with the UB1.5 DOAS algorithm developed at the University of Bremen. Plotted are the columns retrieved from all individual measurements within a 200-km selection radius around the Zugspitze (grey) as well as a reduced data set (orange) which resulted from application of a cloud clearing scheme. The US 1976 Standard NO_2 VMR profile with the tropospheric part ($<$10 km) set to zero was used for airmass factor calculations, assuming no aerosols and a surface albedo of 5%.

quantitative terms. This behavior will be characterized in more detail in the sensitivity study given in Sect. 5.2.

3.5 Pollution clearing for SCIAMACHY data

We saw from Fig. 6, that within the 200-km selection radius around the Zugspitze for a considerable fraction of days regional pollution "hot spots" are included resulting in occasionally high spikes in our data set. The question arises how to detect such regionally polluted pixels in order to obtain a reduced SCIAMACHY data set that is a good measure for the clean background (free) troposphere. Such a "pollution clearing" is a prerequisite for the comparison with Zugspitze FTIR measurements which are essentially not impacted by pollution due to the high altitude location and the properties of the FTIR averaging kernels (see Sect. 5.2).

As shown in Richter et al. (2004) selecting satellite data for the lowest value observed around a station on each day can improve the agreement between satellite and ground-based measurements in polluted situations. However, such a selection will always introduce a low bias. Furthermore, this would lead to a significant reduction of available data, and, thus to worse comparison statistics. Therefore, we apply a refined pollution-clearing approach that intends to compensate for the low bias introduced by a simple minimum selection. It is based on the assumption that the individual minimum column values, that are representative for a clean background (free) troposphere, are impacted by scatter due to the statistical errors of the satellite measurement. Therefore we try to include also higher "minimum values" that are within this scatter bandwidth. The resulting pollution-clearing scheme is performed in 3 steps as follows.

Step 1. A fit to the daily minimum values is performed (Fig. 7a). See Appendix A, for the analytic function used. This fit is restricted to days with $>$6 column measurements within the 200-km selection radius around the Zugspitze, in order to avoid including polluted data to the series of minimum values. Using only days with several measurements increases the probability that the smallest of these measurements is not affected by boundary layer pollution. The threshold minimum number of 6 pixels available per day was retrieved from a statistical (elbow type) distribution plot of the difference between the average column and minimum column for each day against the number of measurements available for that day. For high numbers the difference shows a small scatter around a stable value of $\approx$1 E+15 cm^{-2}, while for smaller numbers it is collapsing towards zero. The minimum number of 6 used for our subsequent analysis was read out via eye from the elbow corner of this scatter plot.

Step 2. In order to eliminate the annual cycle we subtract the fit function result from step 1, see orange points in Fig. 7b for the result. Then we remove all columns that exceed a value of 2 times the average columns value. The result is shown by marine points in Fig. 7b. One iteration is performed (bright blue points), i.e., a cut off at 2 times the average of the marine points (red line in Fig. 7b). Using 2 times the average as a cutoff criterium is an ad hoc approach to achieve our goal of eliminating few but extremely spiking maximum values from an ensemble with rather uniform minimum values.

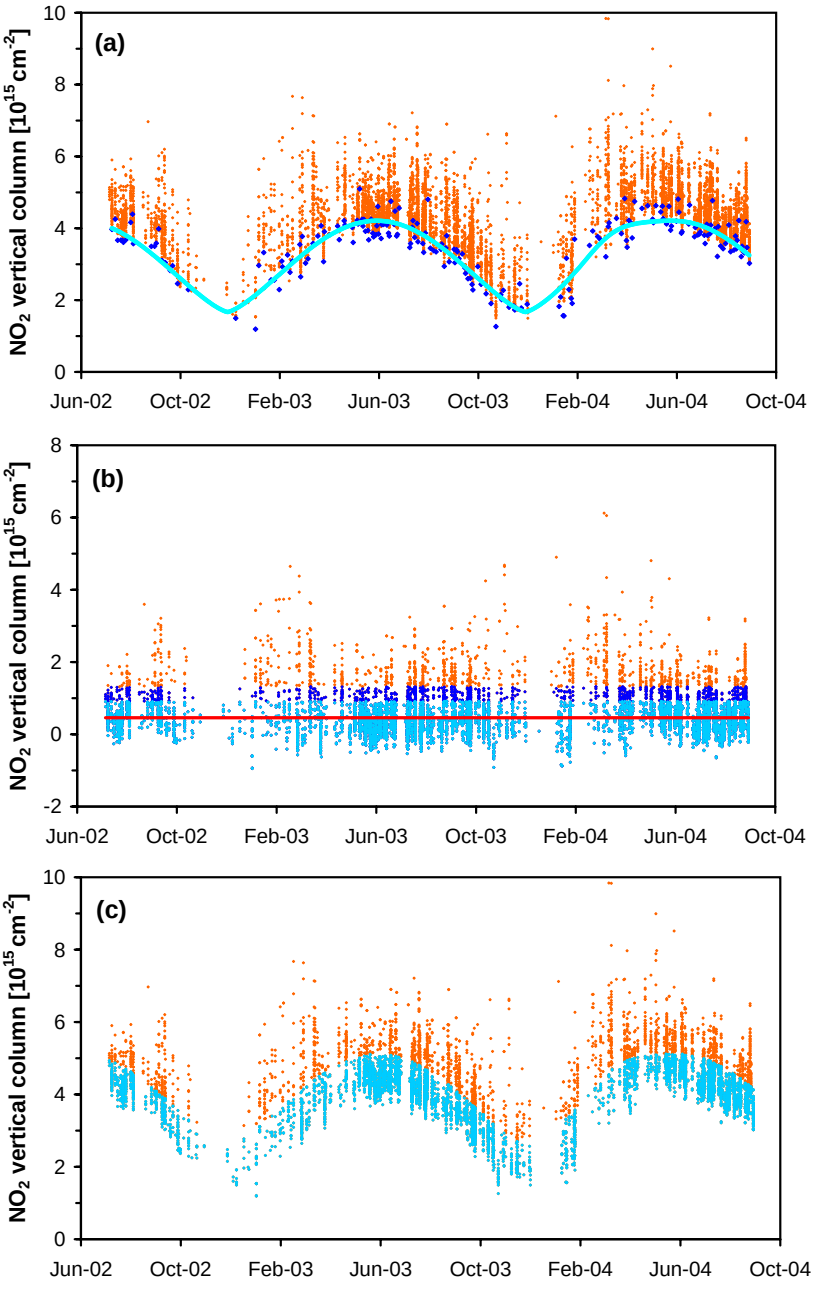

Fig. 7. Orange points: the SCIAMACHY NO_2 vertical column data set analyzed with the UB1.5 DOAS algorithm developed at the University of Bremen. Plotted are columns retrieved from individual measurements within a 200-km selection radius around the Zugspitze. The 3 steps of the pollution clearing for SCIAMACHY data in a 200-km radius around Zugspitze are: **(a)** Fit (blue line) to minimum values (marine). **(b)** Substraction of the fit function result (orange); data cut off at 2 times the average columns value of orange points (marine); one iteration (bright blue) based on average value of marine points (red line). **(c)** Adding of the fit function result from (a) yields final pollution corrected data (bright blue).

Step 3. Adding of the fit function (result from step 1) yields final pollution-cleared data including the annual cycle again (bright blue points in Fig. 7c).

Calculating daily averages of the pollution-cleared data leads to the SCIAMACHY time series shown in Fig. 5 (orange points). A functional fit (orange line) was then performed as described in Appendix A.

Finally, we note that our 3-step approach is just a simple attempt to select data that are representative for clean background conditions in the troposphere, i.e., for days where the

tropospheric VMR could be assumed to be constant throughout the (free) troposphere. We will present an indirect validation of our pollution-clearing approach in the following section.

3.6 Characterization of the daily scatter of SCIAMACHY NO_2 columns

Here we want to give statistical numbers on the NO_2 columns scatter for individual and daily-mean data from our pollution-cleared SCIAMACHY data set (Table 2). Although the statistical quantities are identical to our treatment of FTIR before, we point to the fact that the physical origin of the scatter on the daily scale is dominated by different processes, i.e., the diurnal cycle for FTIR and the inclusion of polluted pixels in the 200-km SCIAMACHY selection radius. Although we performed corrections for both effects, the statistical numbers retrieved from the corrected data sets are probably still residually impacted by these effects.

First we want to characterize the scatter of individual SCIAMACHY column measurements within one day. We derive statistical quantities from the pollution corrected data. For each day (overpass) with index i and n_i measurements within the 200-km selection radius around Zugspitze, the standard deviation σ_i and the standard deviation of the mean value σ_i/sqrt(n_i) were calculated, and subsequently the average of theses quantities over all days derived. The resulting average $AV_i(\sigma_i)$=6.8% is a measure for the scatter of the individual pollution-cleared column measurements.

This result of 6.8% for the precision of an "individual pixel" SCIAMACHY column measurement from investigating pollution corrected data is in agreement with results from a completely independent approach given by Richter et al. (2004): The precision of the column measurements has been assessed to be between 5–10% by analyzing the variability of data over the clean Pacific region which is assumed to be unpolluted in the troposphere. This good agreement shows the validity of our pollution-clearing approach. In other words, the columns that passed our pollution-clearing scheme are obviously a good measure for clean background tropospheric situations, which might by approximated by a constant (free) tropospheric VMR.

$AV_i(\sigma_i/\mathrm{sqrt}(n_i))$=1.9% is a measure for the precision of the daily mean column of SCIAMACHY at the time of overpass within our 200-km selection radius.

Finally, we calculate a standard deviation of the daily columns around the function fitted to the annual cycle (Fig. 5). This leads to a standard deviation of σ=6.5%, see Table 2. This value comprises both the precision of a daily overpass column as well as the day-to-day scatter. It is significantly higher than the precision of a daily overpass average column, which we estimated from $AV_i(\sigma_i/\mathrm{sqrt}(n_i))$=1.9%. Thereby we learn that the true day-to-day scatter for our pollution-clearing criteria and a 200-km radius around Zugspitze is 6.5%.

4 Intercomparison of SCIAMACHY versus FTIR column retrievals

4.1 Intercomparison of scatter

We obtained in Sect. 3.6 a day to-day scatter of 6.5% from SCIAMACHY data with our pollution-clearing criteria applied to a 200-km selection radius around Zugspitze and all resulting data averaged for each day. This agrees well to the FTIR result of 9.2% for the day-to-day scatter. Both data sets are showing sufficient precisions (Table 2) to make the assessment of this ≈10% effect. Note that a perfect agreement could not be expected due to the differing averaging kernels (see Sect. 5.1) and different sampling geometries (Zugspitze point measurement versus SCIAMACHY 200-km selection radius). But this agreement gives again some evidence for the validity of our pollution-clearing scheme.

4.2 Intercomparison of absolute column levels

The difference of the time series of SCIAMACHY and FTIR is displayed in Fig. 5 (red curve). Clearly, the SCIAMACHY columns show significantly higher values throughout the full validation period. The difference (col_{SCIA}–col_{FTIR}) is 0.83 E+15 cm^{-2} on average, with a minimum of 0.60 E+15 cm^{-2} and a maximum of 1.24 E+15 cm^{-2}.

This kind of intercomparison of the direct-output NO_2 column levels from two different remote sounding systems (satellite versus ground) has been performed in many previous papers, and the differences been interpreted in terms of errors of the satellite instrument. However, we would like to point out that this approach is only the first possibility out of two limiting (theoretical) cases: i) The observed differences are due to intrinsic errors in either of the two remote sounding data sets under the simplifying assumption that the two measurement systems have identical sampling characteristics or, ii) the observed difference can be attributed to the different sampling characteristics of the two instruments (differing averaging kernels) under the assumption that they are both working in principle without intrinsic errors. Reality will be in between these limiting cases. A theoretical framework to deal with this problem for the purpose of satellite validation has been given by Rodgers and Connor (2003).

We decided to thereafter follow the assumption ii) as a basis for our subsequent synergistic use of SCIAMACHY and FTIR data aiming at the retrieval of tropospheric NO_2. I.e., we assume the difference shown in Fig. 5 is dominated by the differing sensitivities of SCIAMACHY versus FTIR and not by intrinsic errors of SCIAMACHY (or FTIR) measurements. Clearly, this is a simplifying assumption for the purpose of this study, and future validation studies have to be performed in order to explore to which degree this assumption holds. Our concepts of "virtual coincidence" and "pollution clearing" can contribute to the required refined validation studies.

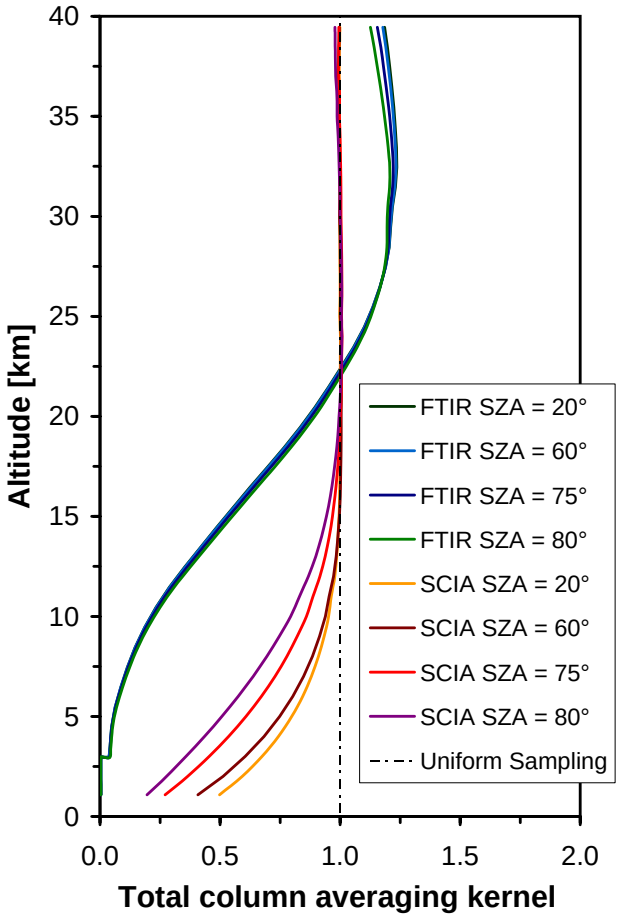

Fig. 8. Total column averaging kernels for Zugspitze FTIR (blue to green lines) and SCIAMACHY UB1.5 NO_2 retrievals (pink to orange lines) calculated for solar zenith angles (SZA) between 20° and 80°. Both FTIR and satellite retrievals are based upon the US 1976 Standard NO_2 VMR a priori profile with the tropospheric part set to zero up to 10 km altitude.

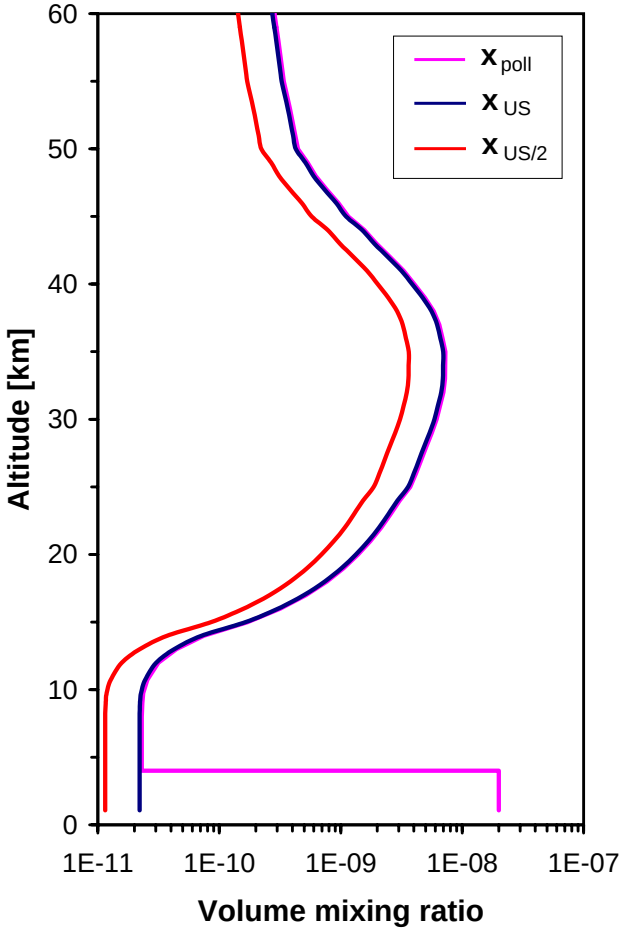

Fig. 9. Three different assumed NO_2 VMR profiles used in a sensitivity study to compare the FTIR versus SCIAMACHY retrievals, see text. Blue: US 1976 Standard NO_2 VMR a priori profile; red: same as blue but all VMR values scaled by a factor of $\frac{1}{2}$; magenta: same as blue, but with enhanced tropospheric VMR of 20 ppbv up to 4 km altitude.

5 Combined FTIR and SCIAMACHY retrieval

In the following we make the simplifying assumption that both FTIR and SCIAMACHY are operating without intrinsic errors and show how additional independent (tropospheric) information can be gained from a combined FTIR plus SCIAMACHY retrieval.

5.1 Total column averaging kernels for the stand-alone FTIR and SCIAMACHY retrievals

Total column averaging kernels are vectors of the dimension of the number of layers or levels of the model atmosphere used, and are thereafter referred to as $\boldsymbol{a}_{\mathrm{FTIR}}$ and $\boldsymbol{a}_{\mathrm{SCIA}}$, respectively. Each vector component stands for a certain altitude and describes to what extent a perturbation of the true VMR profile at a certain altitude relative to the a priori profile used will be reflected in the retrieved total columns, or be underestimated, or overestimated, respectively by the retrieval. An ideal remote sounding system is described by $\boldsymbol{a}^T_{\mathrm{ideal}}$=(111...1), numbers smaller than one would quantify underestimations of true perturbations, numbers above one overestimations. A mathematical description and practical details for total column kernel computations were given for FTIR previously, and can be found, e.g., in Sussmann (1999), and have been given for DOAS only recently for the first time by Eskes and Boersma (2003).

Figure 8 shows the total column averaging kernels for both the Zugspitze FTIR and the SCIAMACHY UB1.5 NO_2-column retrievals. The kernels indicate that both FTIR and SCIAMACHY retrievals perform with a significant underestimation of the tropospheric column, but are able to properly monitor changes in the stratospheric part. Figure 8 shows also differences, namely, i) the underestimation of the

Table 3. Results for the ratio of retrieved columns col_{ret} to the true columns col_{true} computed by Eq. (1), using the averaging kernels shown in Fig. 8 for SZA=60°, and the same a priori profile $\boldsymbol{x}_a$, namely the US Standard NO_2 profile with the tropospheric part up to 10 km set to zero. Three different scenarios are given for the assumed true NO_2 profile $\boldsymbol{x}_{\text{true}}$ as shown in Fig. 9. Scenario 1) $\boldsymbol{x}_{\text{true}}=\boldsymbol{x}_{US}$, i.e., the US Standard NO_2 profile; scenario 2) $\boldsymbol{x}_{\text{true}}=\boldsymbol{x}_{US/2}$, i.e., the US Standard NO_2 profile with all VMR values scaled by a factor of 1/2; scenario 3) $\boldsymbol{x}_{\text{true}}=\boldsymbol{x}_{\text{poll}}$, i.e., $\boldsymbol{x}_{US}$ but with a constant enhanced VMR value of 20 ppbv up to 4 km altitude. For the columns-ground altitude we used 1.077 km a.s.l., which is the average ground altitude within a 200-km radius around the Zugspitze. Examples are given for the Zugspitze FTIR (at 2.964 km a.s.l.) as well as theoretical numbers calculated for a FTIR at 1.077 km a.s.l.

	Zugspitze FTIR @ 2.964 km a.s.l.			FTIR @ 1.077 km a.s.l.	SCIAMACHY		
Scenario	1	2	3	3	1	2	3
$\boldsymbol{x}_{\text{true}}$	$\boldsymbol{x}_{US}$	$\boldsymbol{x}_{US/2}$	$\boldsymbol{x}_{\text{poll}}$	$\boldsymbol{x}_{\text{poll}}$	$\boldsymbol{x}_{US}$	$\boldsymbol{x}_{US/2}$	$\boldsymbol{x}_{\text{poll}}$
$\frac{col_{\text{true}}\ (1.077-10\,\text{km})}{col_{\text{true}}\ (1.077-100\,\text{km})}$	0.053	0.053	0.955	0.955	0.053	0.053	0.955
$\frac{col_{\text{ret}}\ (1.077-100\,\text{km})}{col_{\text{true}}\ (1.077-100\,\text{km})}$	0.950	0.949	0.058	0.078	0.984	0.984	0.570
$\frac{col_{\text{ret}}\ (1.077-100\,\text{km})}{col_{\text{true}}\ (10-100\,\text{km})}$	1.003	1.002	1.239	1.656	1.039	1.039	12.54

tropospheric column is much more pronounced for the FTIR retrieval compared to the satellite retrieval, and, ii) there is a significant zenith-angle dependence of the tropospheric sensitivity in case of the satellite retrieval, but not for the FTIR retrieval.

5.2 Smoothing of tropospheric pollution

In this section, the smoothing effect of the averaging kernels of FTIR and SCIAMACHY (i.e., the under-/overestimation of the true column by the retrievals) is illustrated by a sensitivity study. We assume 3 different scenarios for the true vertical profiles $\boldsymbol{x}_{\text{true}}$ (profile vectors are referred to as $\boldsymbol{x}$, with units either in VMR or partial columns) which all differ in a characteristic manner from the a priori profile $\boldsymbol{x}_a$ (i.e., the reduced US Standard NO_2 profile). The profiles for the 3 scenarios are shown in Fig. 9. Scenario 1 is for $\boldsymbol{x}_{\text{true}}=\boldsymbol{x}_{US}$, i.e., the US Standard NO_2 profile; scenario 2 uses $\boldsymbol{x}_{\text{true}}=\boldsymbol{x}_{US/2}$, i.e., the US Standard NO_2 profile with all VMR values scaled by a factor of 1/2; scenario 3 is based upon $\boldsymbol{x}_{\text{true}}=\boldsymbol{x}_{\text{poll}}$, i.e., $\boldsymbol{x}_{US}$ but with a enhanced VMR value of 20 ppbv up to 4 km altitude. This scenario is derived from typical maximum NO_2 values found from Zugspitze in situ measurements during strong pollution episodes. Such extreme pollution enhancements would not be caused by the uplift of the alpine boundary layer above the Zugspitze altitude that can occasionally happen during summer, but would typically occur during fast frontal passages that contain pollution originating from highly industrialized areas in northern Germany or Czechia (Scheel, personal communication, 2005). The possibility of long range transport of NO_2 has been confirmed from back trajectory calculations (Stohl et al., 2003), and has been identified in GOME measurements (Schaub et al., 2005).

We have listed in Table 3 for FTIR and SCIAMACHY for all 3 scenarios numbers for the ratio of the retrieved column col_{ret} to the true column col_{true}, which can be calculated directly from the averaging kernels, the assumed true profile, and the a priori profile:

$$\frac{col_{\text{ret}}}{col_{\text{true}}} = \frac{\boldsymbol{a}^T(\boldsymbol{x}_{\text{true}}-\boldsymbol{x}_a)+\boldsymbol{a}_{\text{ideal}}^T\boldsymbol{x}_a}{col_{\text{true}}}$$

with

$$col_{\text{true}} = (111...1)\,\boldsymbol{x}_{\text{true}} = \boldsymbol{a}_{\text{ideal}}^T\boldsymbol{x}_{\text{true}}. \quad (1)$$

Table 3 contains also the analogous columns ratio with respect to the true stratospheric part above 10 km. Note that for the column-ground altitudes we used 1.077 km a.s.l., which was retrieved as an average altitude for the 200-km radius around the Zugspitze from a global 1 km×1 km elevation data set (Hastings and Dunbar, 1999). The results of Table 3 are discussed as follows.

Scenario 1. This scenario ($\boldsymbol{x}_{\text{true}}=\boldsymbol{x}_{US}$) describes a clean atmosphere, i.e., the tropospheric column (<10 km) is small compared to the total column (columns ratio 0.053). In this case the column retrieved by Zugspitze FTIR is slightly underestimating the true total column above 1.077 km a.s.l. (factor 0.950) and very weakly overestimating the true stratospheric column (factor 1.003). The underestimation of the true total column is even smaller for SCIAMACHY (factor 0.984) but the overestimation of the stratospheric column is slightly stronger (factor 1.039). The fact that these under-/overestimations are small can be understood by the fact that $\boldsymbol{x}_{\text{true}}$ is identical to $\boldsymbol{x}_a$ in the stratospheric part, and close to $\boldsymbol{x}_a$ within the tropospheric part (<10 km), where the components of $\boldsymbol{x}_a$ are zero, and VMR values of $\boldsymbol{x}_{US}$ are very small.

Scenario 2. This scenario ($\boldsymbol{x}_{\text{true}}=\boldsymbol{x}_{US/2}$) is to test whether a significant scaling factor with respect to $\boldsymbol{x}_a$ is properly reflected by the retrievals for a clean atmosphere. The answer is yes, the numbers are nearly identical to scenario 1. This can be directly understood for the FTIR retrieval, because a profile scaling retrieval is in principle always able to perfectly reflect true atmospheric changes relative to the a priori which can be modeled by one simple scaling factor. (This is only approximately correct in our case because the a priori profile is the reduced US Standard profile, and this leads to the slight deviations of the ratios from unity as in Scenario 1). This also holds for the DOAS retrieval of SCIAMACHY data, as for an optically thin atmosphere the airmass factor does not depend on the NO_2 column but only on the profile shape.

Scenario 3. This scenario ($\boldsymbol{x}_{\text{true}}=\boldsymbol{x}_{\text{poll}}$) is to test to what extent strong boundary layer tropospheric pollution that reaches up to an altitude of 4 km is reflected by the retrievals of FTIR and SCIAMACHY. In this scenario the tropospheric column makes up a considerable fraction of the total column (columns ratio 0.955). Table 3 shows that the Zugspitze FTIR retrieval is nearly insensitive to the tropospheric pollution (factor 0.058), and the retrieved column still can be used as a measure for the pure stratospheric column with a moderate overestimation (factor 1.239). We like to point to a principal advantage of a high-mountain-site FTIR over a ground-level FTIR station, if the target quantity is the pure stratospheric column: For Zugspitze the pollution perturbation (Fig. 9) extends only between 2.964 km and 4 km and thus makes up only a smaller fraction of the total column compared to a FTIR that would be located, e.g., at 1.077 km, where the pollution perturbation would extend from 1.077–4 km. Consequently, together with the fact that the FTIR averaging kernels are showing small values around 0.03 in the altitude range up to 4 km, in case of pollution, the true stratospheric column would be significantly stronger overestimated by a FTIR located at 1.077 km (factor of 1.656 in Table 3) compared to the estimate of the stratospheric column by the Zugspitze mountain site FTIR (overestimation only by a factor of 1.239, see Table 3). We will make use of this advantage of a mountain-site FTIR in the combined retrieval with FTIR and SCIAMACHY below.

The SCIAMACHY retrieval is more sensitive to pollution than FTIR but still significantly underestimates the pollution enhancement (factor 0.570). The retrieved SCIAMACHY column can no longer be used as a measure for the pure stratospheric column under polluted conditions (overestimation by a factor of 12.54).

5.3 Set-up of the combined retrieval

The result of the choice of a common a priori with the tropospheric part set to zero together with the averaging kernels given in Fig. 8 is, that both remote sounding systems will always underestimate the true column since the true atmosphere will always contain a larger tropospheric column than given by the a priori. The corresponding underestimation by SCIAMACHY will be less pronounced since its averaging kernels are closer to unity in the troposphere (Fig. 8). Together with the fact that both FTIR and SCIAMACHY are sampling the stratosphere properly (kernels close to unity, see Fig. 8) the following behavior can be expected for applying the appropriate averaging-kernel based corrections for the tropospheric underestimations to both FTIR and SCIAMACHY: For an iteratively increased assumed true tropospheric column (stratospheric column fixed to a realistic value), there will be a distinct level reached, where the corrected FTIR and SCIAMACHY columns will match together. This is because the correction is always larger for FTIR which starts at lower columns. In other words, the different tropospheric sensitivities of the SCIAMACHY versus FTIR kernels allow for the retrieval of tropospheric NO_2 by combining the two sounding systems. Our approach thereafter is to actually perform such a combined FTIR-SCIAMACHY retrieval of tropospheric NO_2. If the result for troposheric NO_2 compares reasonably well with our a priori knowledge of background clean air levels of tropospheric NO_2, then we have no reason to assume that there is an intrinsic error in either of the sounding systems. Before we give a theoretical formulation of the described procedure we want to note, that this is a sensitivity study in a sense that we do not investigate other possible biasing contributions like the impact of albedo, clouds or aerosols on the SCIAMACHY retrievals.

From our discussion of the differing averaging kernels (Fig. 8) we assume for the combined retrieval by FTIR and SCIAMACHY that we can roughly obtain two independent pieces of information, i.e., stratospheric and tropospheric information. The definition of the corresponding two retrieval parameters are illustrated in Fig. 10, namely, a factor λ_1 for scaling of our (stratospheric) a priori profile $(VMR_a)_i$, and an iterative change of the tropospheric volume mixing ratio VMR_{trop} which is assumed to be constant with altitude. The interconnection of these (stratospheric and tropospheric) parts of the profile is done at their actual crossing point which is, consequently, variable in VMR and altitude.

We write the following two relations for the differences between the column inferred from the combined retrieval col_{combi}, the column retrieved by FTIR col_{FTIR}, and the column retrieved by SCIAMACHY col_{SCIA} (all plotted in Fig. 11a)

$$\begin{aligned} & col_{\text{FTIR}} - col_{\text{combi}} \\ & = col_{\text{FTIR}} - \boldsymbol{a}^T_{\text{ideal}} \cdot \boldsymbol{x}_{\text{combi}} \\ & = \boldsymbol{a}^T_{\text{FTIR}} \cdot (\boldsymbol{x}_{\text{combi}} - \boldsymbol{x}_a) + \boldsymbol{a}^T_{\text{ideal}} \cdot \boldsymbol{x}_a - \boldsymbol{a}^T_{\text{ideal}} \cdot \boldsymbol{x}_{\text{combi}}, \end{aligned} \quad (2)$$

and

$$col_{\text{SCIA}} - col_{\text{combi}}$$

$$= col_{\mathrm{SCIA}} - \boldsymbol{a}^T_{\mathrm{ideal}} \cdot \boldsymbol{x}_{\mathrm{combi}}$$
$$= \boldsymbol{a}^T_{\mathrm{SCIA}} \cdot (\boldsymbol{x}_{\mathrm{combi}} - \boldsymbol{x}_a) + \boldsymbol{a}^T_{\mathrm{ideal}} \cdot \boldsymbol{x}_a - \boldsymbol{a}^T_{\mathrm{ideal}} \cdot \boldsymbol{x}_{\mathrm{combi}}, \quad (3)$$

where the vectors $\boldsymbol{x}$ stand for partial columns profiles.

Our a posteriori retrieval constraint is set up as follows

$$\boldsymbol{x}_{\mathrm{combi}} = \lambda_1 \cdot \boldsymbol{x}_a + \boldsymbol{x}_{\mathrm{trop}} \quad (4)$$

with

$$\boldsymbol{x}_{\mathrm{trop}} = \begin{pmatrix} VMR_{29} \cdot AMF_{29} \\ : \\ VMR_1 \cdot AMF_1 \end{pmatrix}$$

with

$$VMR_i = \begin{cases} 0 \text{ if } VMR_{\mathrm{trop}} < \lambda_1 (VMR_a)_i \\ VMR_{\mathrm{trop}} - \lambda_1 (VMR_a)_i \text{ if } VMR_{\mathrm{trop}} \geq \lambda_1 (VMR_a)_i \end{cases} \quad (5)$$

This describes our retrieval with the two parameters λ_1 and VMR_{trop} (Fig. 10). AMF_i are the infrared airmass factors (i.e., the partial air columns of the different layers) which – multiplied by VMR – give the partial columns profile $\boldsymbol{x}$.

Our retrieval constraint is set up from two parameters, i.e., it allows for retrieval of two independent degrees of freedom, because this is what can be expected from using two complementary input parameters, namely col_{FTIR} and col_{SCIA}. The constraint for the stratospheric part is a simple scaling of the US standard profile as used also for the FTIR retrieval. For the lower part we use a scaling of a VMR profile that is constant with altitude. This is because only one degree of freedom is left for this lower part, and it is the zero-order approach in our case where no better a priori information on the vertical distribution of free tropospheric background NO_2 is available. Our approach of linking the two parts of the profile together just at the point where the tropospheric VMR matches the US standard profile is the simplest solution that avoids (unphysical) negative VMR gradients at the transition between the lower and upper part of the profile.

We derive a starting value for λ_1 by using

$$col_{\mathrm{FTIR}} - col_{\mathrm{combi}} \quad (10-100\,\mathrm{km})=0, \quad (6)$$

because FTIR is a good measure for the true pure stratospheric column. This assumption has been tested in Sect. 5.2 and turned out to hold to a very good approximation.

From Eqs. (2), (4) and (6) it follows

$$\lambda_1 = \frac{col_{\mathrm{FTIR}}}{\boldsymbol{a}^T_{\mathrm{ideal}} \cdot \boldsymbol{x}_a}. \quad (7)$$

For the given λ_1 we subsequently apply the retrieval equation

$$col_{\mathrm{FTIR}} - col_{\mathrm{SCIA}} = (\boldsymbol{a}_{\mathrm{FTIR}} - \boldsymbol{a}_{\mathrm{SCIA}})^T [(\lambda_1 - 1)\boldsymbol{x}_a + \boldsymbol{x}_{\mathrm{trop}}] \quad (8)$$

which describes the iteration of VMR_{trop} via $\boldsymbol{x}_{\mathrm{trop}}$, see Eq. (5) to match the measured columns difference col_{FTIR}–col_{SCIA}.

The resulting tropospheric mixing ratio VMR_{trop} is plotted as a time series in Fig. 11b, and is converted to the tropospheric column (1.077–10 km) within the same figure.

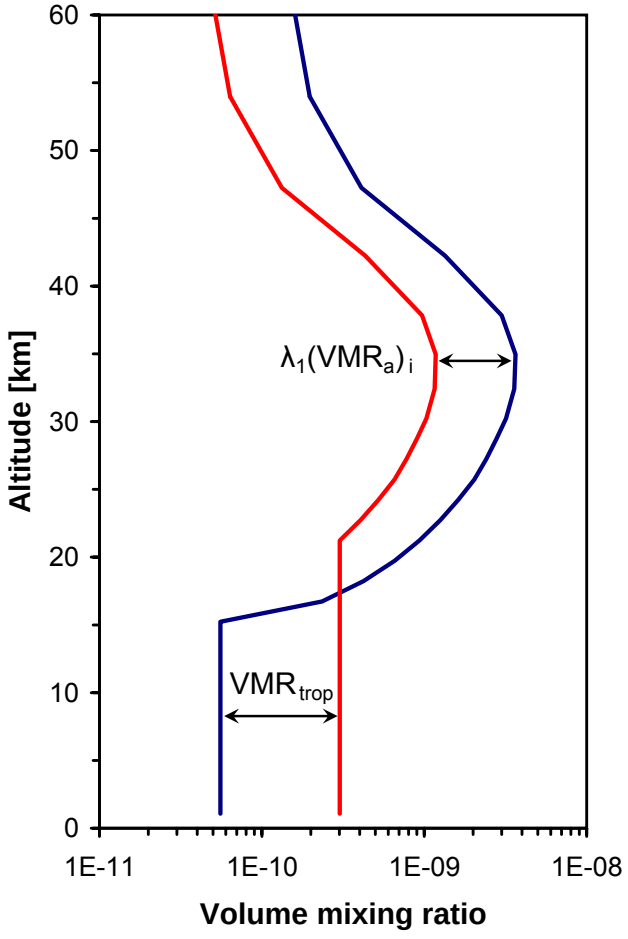

Fig. 10. Schematics for the combined NO_2 retrieval from Zugspitze FTIR and SCIAMACHY using two fitting parameters. First parameter is a scaling factor λ_1 applied to $(VMR_a)_i$, i.e., the US Standard NO_2 a priori profile (with the tropospheric part set to zero). Second fit parameter is the tropospheric volume mixing ratio VMR_{trop} assumed to be constant with altitude. Note that the crossing point between both parts of the profile is variable in VMR and altitude.

Before discussing this result in terms of validation and in geophysical terms, we want to parenthesize two technical remarks.

i) Some scatter in Fig. 11b seems to be in contrast to the smooth functions that have been fitted to FTIR and SCIAMACHY in Fig. 11a. The reason is that for the conversion from VMR to partial column profiles the real pressure-temperature profiles from same-day Munich radio soundings were used (for both FTIR and SCIAMACHY).

ii) For the corrections via averaging kernels a look up table of 25 different averaging kernels was used for 25 different SZA for SCIAMACHY. Thereby the annual cycle of the SZA at satellite overpass and its impact on the relieved columns via the averaging kernels is properly accounted for. For FTIR only one averaging kernel was used (SZA=60°) due to the small zenith angle dependence (see Fig. 8).

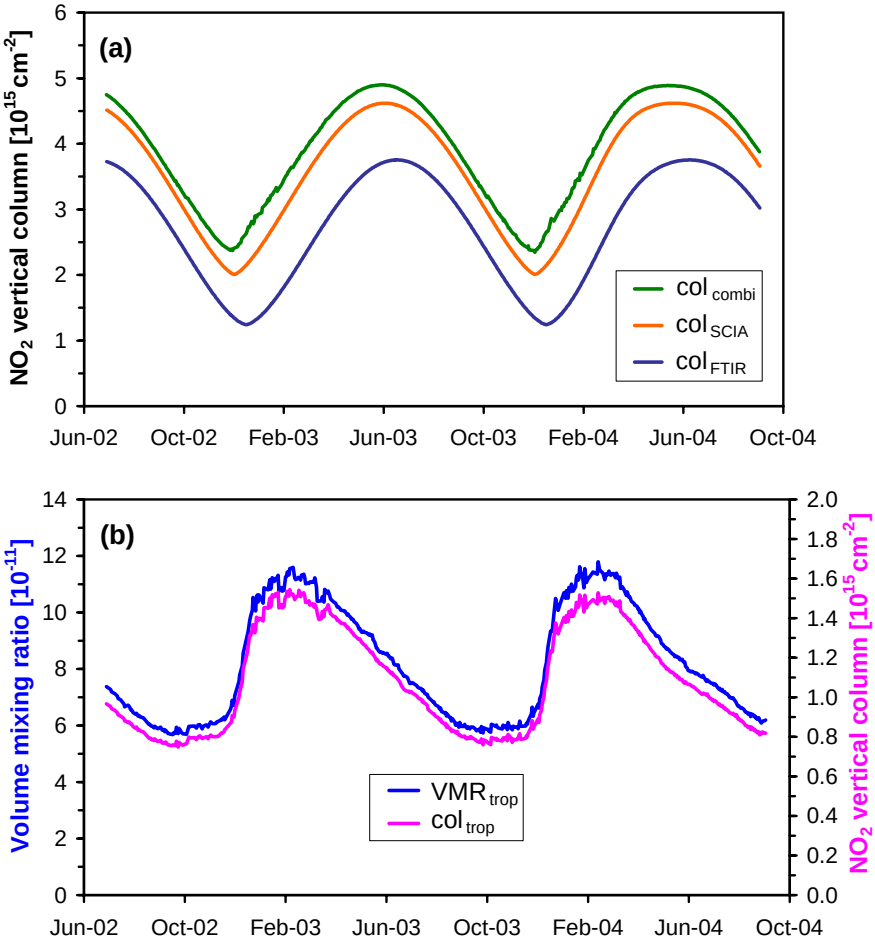

Fig. 11. **(a)** Total column series col_{combi} (green) inferred from the combined a-posteriori retrieval from FTIR and SCIAMACHY data. Column series retrieved from SCIAMACHY alone col_{SCIA} (orange, same as in Fig. 5) and the column series retrieved from FTIR alone col_{FTIR} (blue, same as in Fig. 5). **(b)** Time series of the clean backround tropospheric mixing ratio VMR_{trop} obtained from the combined retrieval of FTIR and SCIAMACHY (blue), and the corresponding clean background tropospheric column between 1.077 km–10 km (col_{trop}, magenta).

5.4 Partial column averaging kernels for the combined retrieval

In Fig. 12 the partial column averaging kernels are displayed for the combined retrieval by FTIR and SCIAMACHY. They have been calculated by the perturbation approach (see, e.g., Sussmann, 1999) around a typical atmospheric state obtained from the retrievals of the whole time series of this study. One kernel has been calculated for the tropospheric column (1.077–10 km). The kernel for the stratospheric column (10–100 km) of the combined retrieval (Fig. 12) is identical to the total column kernel of the stand-alone FTIR retrieval (Fig. 8). This is a logical consequence of our retrieval set up. These two kernels are showing that two independent pieces of information are obtained by the combined retrieval for the troposphere, and stratosphere, respectively. Note that the tropospheric kernel is able to perfectly monitor possible changes within the free troposphere, but shows a significant underestimation of possible changes in the boundary layer. The same effect can be seen from the total column averaging kernel of the combined retrieval (Fig. 12).

5.5 Discussion of the retrieved tropospheric columns series in terms of validity

First of all, Fig. 11b shows that the retrieved tropospheric columns (1.077 km–10 km) are showing a pronounced annual cycle. It displays a minimum of 0.75 E+15 cm^{-2}, a maximum of 1.54 E+15 cm^{-2}, and an average of 1.09 E+15 cm^{-2}. As discussed earlier in this paper, due to our pollution-clearing criteria, our results should be a measure for clean tropospheric background conditions. For such clean background conditions, columns of the order of 1–3 E+15 were frequently observed by ground-based UV/vis

measurements during a recent extensive validation study of GOME tropospheric nitrogen dioxide in the Po basin (Petritoli et al., 2004). Thus, we have evidence that the tropospheric columns retrieved from combined FTIR and SCIAMACHY retrievals are within a reasonable range of magnitude. This is only a qualitative statement and it means that from our findings we can neither exclude nor find any evidence for an intrinsic principle error in the SCIAMACHY data set.

We repeat, however, that the UB1.5 algorithm was empirically tuned by adding 1.0 E+15 cm^{-2} to the slant columns, which translates to a vertical column offset of 0.05–0.5 E+15 cm^{-2} depending on season (Richter et al., 2004). Due to limited a priori knowledge of the clean background tropospheric NO_2 column (see above) we cannot decide from this study whether this empirical correction to SCIAMACHY has to be refined or not.

A more quantitative validation of our new method could be performed in an upcoming study using collocated SCIAMACHY tropospheric columns retrieved with the Richter and Burrows (2002) method. In fact the two methods are independent (because now the stratospheric background to be removed is that of FTIR and not that retrieved by SCIAMACHY over the Pacific Ocean) so that useful indications on selfconsistency and/or validation of the new approach (or limitations of the old one) can be pointed out.

5.6 Discussion of the retrieved tropospheric column in geophysical terms

Now we want to discuss the annual cycle of the background (free) tropospheric columns series which we obtained from the combined retrieval (Fig. 11b), assuming that both FTIR and SCIAMACHY are performing without intrinsic errors. Clearly, the retrieved background free tropospheric columns annual cycle shows a significant phase shift towards earlier times compared to both the stratospheric and the total columns series (col_{FTIR} and col_{combi} in Fig. 11a). On the other hand, the annual cycle of "boundary layer" NO_2 is known to show a symmetric mid-winter maximum due to human fuel combustion related to traffic and heating systems and a broader symmetric summer minimum which is due to the smaller emissions in combination with a reduced NO_2 lifetime in summer (see, e.g., Fig. 6 in Petritoli et al., 2004). Compared to that, our retrieved free tropospheric columns series shows a similar fall-winter increase, but a slower decrease during summer with a minimum in fall. At least the tendency of this delay effect relative to the boundary layer cycle might be tentatively explained by the fact that our retrieved tropospheric columns are representative for the clean (free) troposphere, where the lifetime of NO_2 is significantly higher (up to 10 days) than in the boundary layer (<1 day), see, e.g., IPCC (2001).

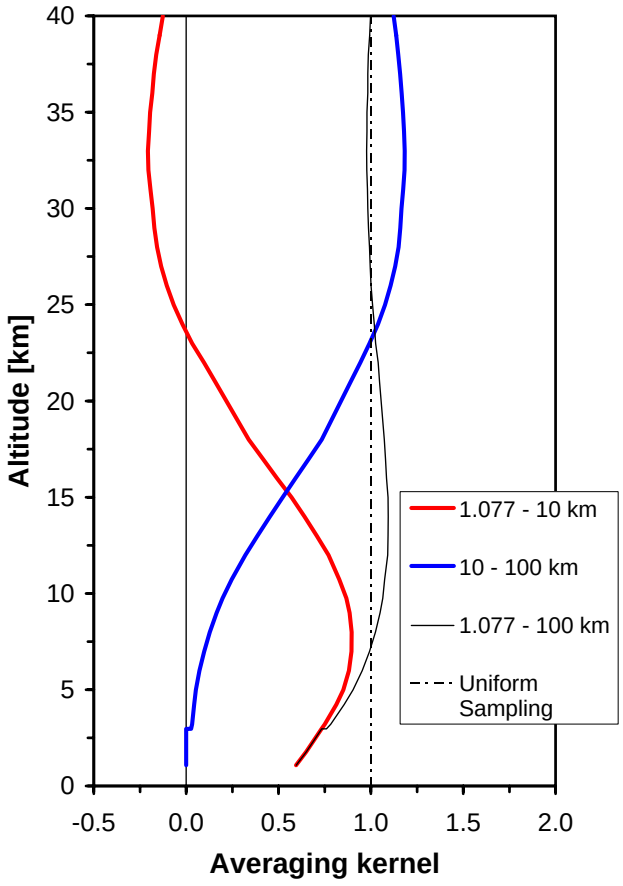

Fig. 12. Averaging kernels for the combined FTIR and SCIAMACHY retrieval of NO_2, calculated for a solar zenith angle of 20°. Red curve: Tropospheric partial column averaging kernel (calculated for 1.077–10 km). Blue curve: Stratospheric partial column averaging kernel (calculated for 10–100 km). Black curve: total column averaging kernel for the combined retrieval.

6 Conclusions and outlook

Columnar NO_2 retrievals from solar FTIR measurements of the time span July 2002–October 2004 were used synergistically with columnar NO_2 retrieved from SCIAMACHY data by the University of Bremen scientific algorithm UB1.5.

We have presented several new concepts for the data matching between FTIR and satellite measurements of columnar NO_2 for the purpose of validation and synergistic use. A new approach was presented to account for the daytime increase of stratospheric NO_2 and match FTIR data to the time of satellite overpass. This is performed by constructing "virtual coincidences" that make use of the NO_2 daytime increasing rate retrieved from the FTIR data set itself [+1.02(6) E+14 cm^{-2}/h]. The measured increasing rate shows no significant seasonal variation for our midlatitude data set. This is in contrast to results from stratospheric photochemical model calculations. A pollution-clearing scheme

for the SCIAMACHY data was developed to select only pixels corresponding to clean background (free) tropospheric conditions and thus to exclude local pollution hot spots within the 200-km selection radius around the Zugspitze. Furthermore, a generic analytic function was designed in order to better fit obvious deviations of columnar NO_2 annual cycles from a sine function. Thereby statistical properties (day-to-day scatter) can be calculated relative to this fitted annual cycle.

From a direct intercomparison (i.e., without correcting for the different sensitivities) we derived the difference between SCIAMACHY and FTIR columns. It varies between 0.60–1.24 E+15 cm^{-2} with an average of 0.83 E+15 cm^{-2}. A day-to-day scatter of daily means of ≈7–10% could be retrieved in mutual agreement from both FTIR and SCIAMACHY.

We have shown that FTIR gives a nearly unbiased (<25% maximum bias in case of extreme tropospheric pollution, clean air bias <1%) and highly precise measure of the pure stratospheric column (precision of the daily mean or virtual-coincidence column 4.3%). This is achieved by using measurements from a mountain station, which is located above the possibly polluted boundary layer, and an a priori profile with the tropospheric part set to zero.

Using Zugspitze FTIR soundings set up in this way, we have formulated a combined a posteriori retrieval of FTIR and SCIAMACHY for the tropospheric column, based upon the averaging kernels. This combined retrieval was performed under the simplifying assumption that SCIAMACHY and FTIR are operating without intrinsic errors, i.e., the observed differences between SCIAMACHY and FTIR are only due to tropospheric NO_2. It yields an annual cycle of the clean background (free) tropospheric column (<10 km) with variations between 0.75–1.54 E+15 cm^{-2}, an average of 1.09 E+15 cm^{-2}, and an intermediate phase between that of the well known boundary layer and stratospheric annual cycles. Similar column levels have been found from ground-based UV/vis measurements of the background (free) tropospheric column in the Po valley.

Although our combined retrieval was based upon the assumption that both FTIR and SCIAMACHY are operating without errors, there could be some SCIAMACHY errors in reality, of course. However, these errors are minimized by our use of averaging kernels and will only be relevant if the atmospheric conditions deviate strongly from the parameters used in the forward modelling. A validation of our new method could be performed in an upcoming study using collocated SCIAMACHY tropospheric columns retrieved with the Richter and Burrows (2002) reference sector method. Since the two methods are independent useful indications on selfconsistency and/or validation of the new approach could be pointed out.

Our results were shown for our validation application for selected SCIAMACHY pixels without pollution only, but can be also applied to polluted SCIAMACHY data. Our presentation was in the tradition of a point-location time series for the Zuspitze, but can, of course, be converted to a horizontal map of tropospheric NO_2 as well. For this, the averaging kernels have to be determined for each measurement independently using the best estimates for albedo, aerosols, clouds and NO_2 profile available (Eskes and Boersma, 2003).

We have shown how to use a FTIR mountain site as a reference for combined satellite retrievals of tropospheric NO_2 over land. This is a complementary approach in addition to the traditional method using stratospheric reference columns retrieved over sea. The latter is based on the assumption of a longitudinally homeogeneous stratospheric NO_2 layer. Variations can, however, clearly not be neglected close to the Polar Vortex or during major changes in stratospheric dynamics.

Therefore, our result can be transferred to the use of a group of FTIR stations (preferably mountain sites) within the Network of the Detection of Stratospheric Change (NDSC) as "calibration points" for improved global satellite retrievals of tropospheric NO_2 over land. The minimum requirement for such an "integrated global NO_2 observing system" would be one FTIR for a horizontal area for which the stratospheric column can be assumed to be constant to a sufficient degree, e.g., for latitudinal bands towards the Pacific with meridional extensions of several hundreds of kilometers.

Finally, we expect that the concepts described in this study can be transferred to a variety of possible combined a posteriori retrievals of further trace species from satellite and ground-based FTIR systems that might be synergistically exploited in near future.

Appendix A: Analytic function to fit NO_2 columnar annual cycles

A generic analytic function was designed in order to better fit two obvious deviations of columnar NO_2 annual cycles from a sine function. i) Different radii of curvature are observed the minimum and maximum, respectively, and ii) maxima and minima are often delayed or shifted to earlier times, leading to an asymmetry in the peaks and/or minima.

The function is

$$f = b - a + 2a \cdot \left\{ \left[\sin\left(\pi \frac{x - x_0}{365 \cdot \left(1 + c \cdot e^{-\left(\frac{x - x_p}{\sigma}\right)^2} \right)} + \frac{\pi}{4} \right) \right]^2 \right\}^{\gamma} \tag{A1}$$

with the 7 (fitting) parameters a, b, c, x_0, x_p, σ, and γ.

In order to discuss this function we consider 3 cases.

Case 1. γ=1, c=0.

This reduced case is the sine function

$$f_1 = b + a \cdot \sin\left(2\pi \frac{x - x_0}{365} \right) \tag{A2}$$

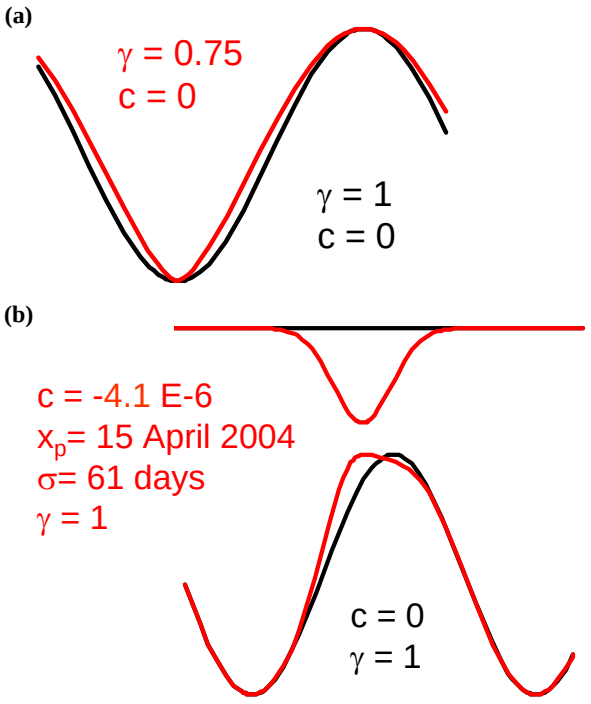

Fig. A1. Schematics to illustrate the analytic function used to fit the annual cycle of NO_2 columns, i.e., its deviations from a sine function. **(a)** Decrease of the radius of curvature around the minimum by using γ (<1) as a fitting parameter. **(b)** Shift of maximum to earlier times by a local Gaussian frequency modulation using as fit parameters the strength c, the position in time x_p, and the width σ.

Case 2. $\gamma<1$, c=0.

This case describes the decreased radius of curvature around the minimum

$$f_2 = b - a + 2a \cdot \left\{ \left[\sin\left(\pi \frac{x - x_0}{365} + \frac{\pi}{4} \right) \right]^2 \right\}^{\gamma}, \qquad \text{(A3)}$$

see Fig. A1a, for an illustration.

Case 3. $c\neq0$, γ=1.

This case describes a local Gaussian frequency perturbation with strength c, position x_p, and width σ

$$f_3 = b + a \cdot \sin\left(2\pi \frac{x - x_0}{365 \cdot \left(1 + c \cdot e^{-\left(\frac{x - x_p}{\sigma}\right)^2} \right)} \right), \qquad \text{(A4)}$$

see Fig. A1b, for an illustration.

Acknowledgements. The authors like to thank the referee, F. Boersma (KNMI), as well as the second, anonymous referee for carefully reading this manuscript and making very helpful suggestions for improvements to this paper. They thank A. Rockmann (IMK-IFU) for maintaining the Zugspitze FTIR measurements and M. Erhard (IMK-IFU) for preparing the elevation-model data set. Basic funding of the Permanent Ground-Truthing Facility Zugspitze/Garmisch is provided by the German Federal Ministry of Education and Research (BMBF) via the Program "Atmosphere and Climate" of the German Helmholtz Association of National Research Centres. Funding by BMBF/DLR as part of the German SCIAMACHY validation program (GCVOS) via contract DLR 50 EE 0007 and by the EC within the project UFTIR (contract EVK2-CT-2002-00159) is gratefully acknowledged. This work contributes to the ESA-ENVISAT-Validation-Project TASTE and is part of the EC-Network of Excellence ACCENT-TROPOSAT-2. SCIAMACHY lv0 and lv1 data were provided by ESA through DLR/DFD.

Edited by: H. Kelder

References

Anderson, G. P., Clough, S. A., Kneizys, F. X., Chetwynd, J. H., and Shettle, E. P.: AFGL Atmospheric constituents Profiles (0–120 km), Air force Geophysical Laboratory, Hanscom, Mass., USA., Report AFGL–TR–86–1001, AD175173, 1986.

Boersma, K. F., Eskes, H. J., and Brinksma, E. J.: Error analysis for tropospheric NO_2-retrival from space, J. Geophys. Res., 109, D04311, doi:10.1029/2003JD003962, 2004.

Borell, P., Borell, P. M., Burrows, J. P., and Platt, U.: TROPOSAT – Sounding the troposphere from space: a new era for atmospheric chemistry, EUROTRAC-2 Subproject Final Report, ISBN 3-8236-1390-1, Springer, 2004.

Bovensmann, H., Burrows, J. P., Buchwitz, M., Frerick, J., Noël, S., Rozanov, V. V., Chance, K. V., and Goede, A.: SCIAMACHY – Mission Objectives and Measurement Modes, J. Atmos. Sci., 56, 127–150, 1999.

Camy-Peyret, C., Flaud, J.-M., Laurent, J., and Stokes, G. M.: First infrared measurement of atmospheric NO_2 from the ground, Geophys. Res. Lett., 10, 35–38, 1983.

Crutzen, P. J.: The role of NO and NO_2 in the chemistry of the troposphere and stratosphere, Ann. Rev. Earth Planet. Sci., 7, 443–472, 1979.

Eskes, H. J. and Boersma, K. F.: Averaging kernels for DOAS total-column satellite retrievals, Atmos. Chem. Phys., 3, 1285–1291, 2003,
SRef-ID: 1680-7324/acp/2003-3-1285.

Flaud, J.-M., Camy-Peyret, C., Cariolle, D., Laurent, J., and Stokes, G. M.: Daytime variation of atmospheric NO_2 from ground-based infrared measurements, Geophys. Res. Lett., 10, 1104–1107, 1983.

Flaud, J.-M., Camy-Peyret, C., Brault, J. W., Rinsland, C. P., and Cariolle, D.: Nighttime and daytime variation of atmospheric NO_2 from ground-based infrared measurements, Geophys. Res. Lett., 15, 261–264, 1988.

Hastings, D. A. and Dunbar, P. K.: Global Land One-kilometer Base Elevation (GLOBE) Digital Elevation Model, Documenta-

tion, Vol.1, National Oceanic and Atmospheric Administration, Report 34, Boulder, Colorado, 1999.

Heland, J., Schlager, H., Richter, A., and Burrows, J. P.: First comparison of tropospheric NO_2 column densitites retrieved from GOME measurements and in situ aircraft profile measurements, Geophys. Res. Lett., 29, doi:10.1029/2002GL015528, 2002.

Heue, K.-P., Richter, A., Bruns, M., Burrows, J. P., Friedeburg, C. v., Platt, U., Pundt, I., Wang, P., and Wagner, T.: Validation of SCIAMACHY tropospheric NO_2-columns with AMAXDOAS measurements, Atmos. Chem. Phys., 5, 1039-1051, 2005, **SRef-ID: 1680-7324/acp/2005-5-1039**.

IPCC, IPCC Third Assessment: Climate Change 2001, The Scientific Basis, Intergovernmental Panel of Climate Change, 2001 (http://www.ipcc.ch/).

Levelt, P. F., van der A, R., Bhartia, P. K., et al.: Science Requirements Document for OMI-EOS, ISBN 90-369-2187-2, KNMI publication 193 (http://www.knmi.nl/omi/documents/science/SRD-Version-2-version-2-of-7-December-2000.pdf), 2000.

Lambert, J.-C., Pommereau, J.-P., Gleason, J. F., et al.: Investigation of Pole-to-Pole Performances of Spaceborne Atmospheric Chemistry Sensors with the NDSC, J. Atmos. Sci., 56, 176–193, 1999.

Lambert, J.-C., Blumenstock, T., Boersma, F., Bracher, A., De Mazière, M., Demoulin, P., De Smedt, I., Eskes, H., Gil, M., Goutail, F., Granville, J., Hendrick, F., Ionov, D. V., Johnston, P. V., Kostadinov, I., Kreher, K., Kyrö, E., Martin, R., Meier, A., Navarro-Comas, M., Petritoli, A., Pommereau, J.-P., Richter, A., Roscoe, H. K., Sioris, C., Sussmann, R., Van Roozendael, M., Wagner, T., Wood, S., and Yela, M.: Geophysical Validation of SCIAMACHY NO_2 Vertical Columns: Overview of Early 2004 Results, in: Proc. ACVE-2 workshop, 3–7 May 2004, ESA-ESRIN, Frascati, Italy, SP-562, 2004.

Lauer, A., Dameris, M., Richter, A., and Burrows, J. P.: Tropospheric NO_2 columns: a comparison between model and retrieved data from GOME measurements, Atmos. Chem. Phys., 2, 67–78, 2002, **SRef-ID: 1680-7324/acp/2002-2-67**.

Leue, C., Wenig, M., Wagner, T., Klimm, O., Platt, U., and Jahne, B.: Quantitative analysis of NO_x emissions from Global Ozone Monitoring Experiment satellite image sequences, J. Geophys. Res., 106, 5493–5505, 2001.

Martin, R. V., Parrish, D. D., Ryerson, T. B., Nicks Jr., D. K., Chance, K., Kurosu, T. P., Jacob, D. J., Sturges, E. D., Fried, A., and Wert, B. P.: Evaluation of GOME satellite measurements of tropospheric NO_2 and HCHO using regional data from aircraft campaigns in the southeastern United States, J. Geophys. Res., 109, D24307, doi:10.1029/2004JD004869, 2004.

Petritoli, A., Bonasoni, P., Giovanelli, G., Ravegnani, F., Kostadinov, I., Bortoli, D., Weiss, A., Schaub, D., Richter, A., and Fortezza, F.: First comparison between ground-based and satellite-borne measurements of tropospheric nitrogen dioxide in the Po basin, J. Geophys. Res., 109, D15, D15307, doi:10.1029/2004JD004547, 2004.

Pougatchev, N. S., Connor, B. J., and Rinsland, C. P.: Infrared measurements of the ozone vertical distribution above Kitt Peak, J. Geophys. Res., 100, 16 689–16 697, 1995.

Richter, A. and Burrows, J. P.: Retrieval of tropospheric NO_2 from GOME measurements, Adv. Space Res., 29, 1673–1683, 2002.

Richter, A., Burrows, J. P., Fietkau, S., Medeke, T., Notholt, J., Oetjen, H., Sierk, B., Warneke, T., Wittrock, F., Dix, B., Friess, U., Wagner, T., Blumenstock, T., Griesfeller, A., Sussmann, R., Rockmann, A., and Schulz, A.: A scientific NO_2 product from SCIAMACHY: First results and validation, in: Proc. ACVE-2 workshop, 3–7 May 2004, ESA-ESRIN, Frascati, Italy, SP-562, 2004.

Rinsland, C. P., Goldman, A., Murcray, F. J., Murcray, R. D., Blatherwick, R. D., and Murcray, D. G.: Infrared measurements of atmospheric gases above Mauna Loa, Hawaii, in February 1987, J. Geophys. Res., 93, 12 607–12 626, 1988.

Rinsland, C. P., Weisenstein, D. K., Ko, M. K. W., Scott, C. J., Chiou, L. S., Mahieu, E., Zander, R., and Demoulin, P.: Post-Mount Pinatubo eruption ground-based infrared stratospheric column measurements of HNO_3, NO, and NO_2 and their comparison with model calculations, J. Geophys. Res., 108, 4437, doi:10.1029/2002JD002965, 2003.

Rodgers, C. D.: Information content and optimisation of high spectral resolution remote measurements, Adv. Space Res., 21, 361–367, 1998.

Rodgers, C. D. and Connor, B. J.: Intercomparison of remote sounding instruments, J. Geophys. Res., 108, doi:10.1029/2002JD002299, 2003.

Rothmann, L. S., Barbe, A., Benner, D. C., Brown, L. R., Camy-Peyret, C., Carleer, M. R., Chance, K., Clerbaux, C., Dana, V., Devi, V. M., Fayt, A., Flaud, J. M., Gamache, R. R., Goldman, A., Jacquemart, D., Jucks, K. W., Lafferty, W. J., Mandin, J. Y., Massie, S. T., Nemtchinov, V., Newnham, D. A., Perrin, A., Rinsland, C. P., Schroeder, J., Smith, K. M., Smith, M. A. H., Tang, K., Toth, R. A., Vander Auwera, J., Varanasi, P., and Yoshino, K.: The HITRAN molecular spectroscopic database: edition of 2000 including updates through 2001, J. Quant. Spectrosc. Radiat. Transfer, 82, 5–44, 2003.

Schaub, D., Weiss, A. K., Kaiser, J. W., Petritoli, A., Richter, A., Buchmann, B., and Burrows, J. P.: A transboundary transport episode of nitrogen dioxide as observed from GOME and its impact in the Alpine region, Atmos. Chem. Phys., 5, 23–37, 2005, **SRef-ID: 1680-7324/acp/2005-5-23**.

Solomon, S., Portmann, R. W., Sanders, R. W., Daniel, J. S., Madsen, W., Bartram, B., and Dutton, E. G.: On the role of nitrogen dioxide in the absorption of solar radiation, J. Geophys. Res., 104, 12 047–12 058, 1999.

Stohl, A., Huntrieser, H., Richter, A., Beirle, S., Cooper, O. R., Eckhardt, S., Forster, C., James, P., Spichtinger, N., Wenig, M., Wagner, T., Burrows, J. P., and Platt, U.: Rapid intercontinental air pollution transport associated with a meteorological bomb, Atmos. Chem. Phys., 3, 969–985, 2003, **SRef-ID: 1680-7324/acp/2003-3-969**.

Sussmann, R. and Schäfer, K.: Infrared spectroscopy of tropospheric trace gases: combined analysis of horizontal and vertical column abundances, Appl. Opt., 36, 735–741, 1997.

Sussmann, R.: Ground-based Fourier transform spectrometry at the NDSC site Zugspitze: Geophysical products for satellite validation, in: Proceedings of the European Symposium on Atmospheric Measurements from Space, ESTEC, Noordwijk, The Netherlands, 18–22 Jan. 1999, WPP-161, 2, 661–664, 1999.

Sussmann, R.: Establishment of an Integrated Ground-Truthing Station for Satellite Data Products (http://troposat.iup.uni-heidelberg.de/AT2/PIs/TG_3/Sussmann.htm), 2004.

Sussmann, R., Stremme, W., Rettinger, M., and Rockmann, A.: Validation of SCIAMACHY Operational Near-Real-Time Level-2 Products by FTIR at the Ground Truthing Station Zugspitze, in: Proc. ACVE-2 workshop, 3–7 May 2004, ESA-ESRIN, Frascati, Italy, SP-562, 2004a.

Sussmann, R., Buchwitz, M., and Richter, A.: Validation of SCIAMACHY Scientific Retrievals of CO, CH_4, N_2O, and NO_2 by FTIR at the Ground Truthing Station Zugspitze, in: Proc. ACVE-2 workshop, 3–7 May 2004, ESA-ESRIN, Frascati, Italy, SP-562, 2004b.

Sussmann, R. and Buchwitz, M.: Initial validation of ENVISAT/SCIAMACHY columnar CO by FTIR profile retrievals at the Ground-Truthing Station Zugspitze, Atmos. Chem. Phys., 5, 1497–1503, 2005,
SRef-ID: 1680-7324/acp/2005-5-1497.

Sussmann, R., Stremme, W., Buchwitz, M., and de Beek, R.: Validation of ENVISAT/SCIAMACHY columnar methane by solar FTIR spectrometry at the Ground-Truthing Station Zugspitze, Atmos. Chem. Phys., 5, 2419–2429, 2005,
SRef-ID: 1680-7324/acp/2005-5-2419.

WMO/CEOS report on a strategy for integrating satellite and ground-based observations of ozone, Committee on Earth Observation Satellites, Global Atmosphere Watch (GAW), report no. 140, World Meteorological Organization, Geneva, 2000.